Article:

ON THE EFFECT OF AMBIENT TURBULENCE AND THERMODYNAMIC CONDITIONS ON FUEL SPRAY DEVELOPMENT FOR DIRECT-INJECTION SPARK-IGNITION ENGINES

P.G. Aleiferis* and Z.R. van Romunde

Department of Mechanical Engineering, University College London, UK

G. Larson, M. Lawes and C.G.W. Sheppard

School of Mechanical Engineering, University of Leeds, UK

*Author for Correspondence:

Dr. Pavlos Aleiferis

University College London

Department of Mechanical Engineering

Torrington Place, London WC1E 7JE, UK

Tel: +44-(0)20-76793862, Fax: +44-(0)20-73880180

E-mail: p.aleiferis@ucl.ac.uk

ABSTRACT

High-pressure multi-hole injectors for direct-injection spark-ignition engines offer certain flexibility in spray directionality by selecting the number and angle of the nozzle's holes to suit the design of a particular combustion chamber. However, the spray's pattern can change significantly for injector-body temperatures representative of real engine operation at low-load conditions with injection strategies in the early intake stroke. This is due to rapid phase change effects from flash boiling of the high-volatility components of gasoline. This work presents results from an optical investigation into the effects of injector-body temperature and back pressure on the pattern of spray formation, especially when coupled to different levels of ambient turbulence. Specifically, gasoline and iso-octane fuels were tested in the range of 20–120 °C injector-body temperatures and for ambient pressures of 0.5–5.0 bar. Additionally, the ambient turbulence was varied in the range 0–4 m/s to observe its effect on flash-boiling and non-flash-boiling sprays. Results from a combination of high-speed shadowgraphy and simultaneous Schlieren and Mie scattering optical techniques are presented in terms of imaged spray areas and plume penetration. Calculations of the Stokes number are also discussed with respect to turbulence and fuel properties. The results demonstrate a marginal effect of the degree of turbulence intensity on non-flash-boiling sprays that maintained their nominal plume directionality throughout the injection event. However, a significant effect on the spray's penetration and mixing at conditions of fuel flash-boiling was observed with increasing levels of turbulence intensity; the collapsed pattern of the spray's formation exhibited much faster dispersion and mixing.

ABBREVIATIONS

ASOI   After Start Of Injection

DISI   Direct Injection Spark Ignition

RON   Research octane Number

RPM   Revolutions Per Minute

SMD   Sauter Mean Diameter

SOI   Start Of Injection

INTRODUCTION

INJECTION SYSTEMS FOR DIRECT-INJECTION SPARK-IGNITION ENGINES

The gasoline Direct-Injection Spark-Ignition (DISI) engine has several practical advantages over the port-fuel injected engine, such as greater precision in fuel metering and significant potential in fuel economy. Other advantages, such as larger charge cooling potential, allow higher engine compression ratios to be used, increasing the thermal efficiency. However, over the last decade it has become clear that successful implementation of these benefits has been more difficult to achieve than originally anticipated. For example, first generation side-injection systems relied on a piston-bowl to achieve the 'stratified charge' concept, but were plagued by pool fires on the piston as the fuel failed to evaporate fully in the time available before ignition, thus producing unacceptable levels of emissions [1]. Other issues related to changes of the spray's shape at different in-cylinder pressures, e.g. spray collapse of pressure-swirl atomizers at high in-cylinder pressure, also necessitated further research [2–5]. Latest design high-pressure multi-hole injectors aim to resolve these issues over a range of combustion chamber geometries and injection strategies by providing spray directionality through a number of nozzle holes designed to deliver the fuel flexibly where necessary, i.e. towards the spark plug or any other in-cylinder area of interest [6–10].

The majority of work published to date on multi-hole injectors concerns Diesel nozzle geometries, with particular experimental features and analysis targeted at this combustion system. The sensitivities to geometrical differences of the injector nozzles and piston design, the varied operating conditions for the DISI combustion system and its particular mixture preparation requirements merit specific attention and are the motives behind continued research in this field. For example, DISI injectors are mounted in the engine head where the fuel inside the injector and the spray upon injection are both subjected to a wide range of temperature and pressure. More specifically, DISI injectors must inject fuel at conditions of low in-cylinder pressure, typically from about 0.2 bar at very low load with early injection strategies for homogeneous mixture formation, to about 5 bar for late-injection strategies under stratified engine operation, or even more under supercharged operation. Additionally, fuel temperatures can vary from well below 0 °C for cold-start engine conditions to over 150 °C at the injector tip under high-load firing conditions. Although quite significant phenomena are coupled over this operation regime, only recently optical studies of multi-hole injectors have presented results with various types of fuels that demonstrate the coupling between in-nozzle cavitation, near-nozzle spray formation, fuel flash-boiling and droplet sizes [11–15]. Additionally, in-cylinder research has demonstrated the effect of tumble flow and injection strategies on spray formation and wall impingement in DISI engines with multi-hole injectors [16–17]. However, in-cylinder air flow is composed of a range of flow scales, e.g. large 'bulk' structures and localised, smaller scale turbulent air motion. Generally, previous work has shown that the large scale bulk flow structures predominantly control the air/fuel mixing and degree of stratification, whilst smaller-scale high-frequency turbulent structures affect the rate of fuel consumption following ignition leading to a turbulent burning velocity that is several times larger than the fuel's laminar burning velocity. The latter has been confirmed in combustion vessels where turbulence levels can be controlled without superimposition of bulk flow structures, i.e. with zero 'mean' flow [18], as well as in engines of various flow configurations [19], including lately DISI engines with multi-

hole injectors [20]. However, the effect of turbulence on spray formation in DISI engines has not been the subject of any major experimental study, therefore, the precise nature of interaction between local flow turbulence and spray development is not well understood. In fact, it is only recently that some research demonstrated the effect of turbulence on pressure-swirl atomisers for DISI engines, but with fuel temperature only at 20 °C [21]. No data exist for multi-hole injectors or at high fuel temperature, low-gas pressure conditions, i.e. when fuel flash boiling leads to spray collapse.

PRESENT CONTRIBUTION

Considering the very limited amount of previous work on this topic, the aim of the present study was to investigate the effects of ambient turbulence on the structure of the spray from a multi-hole fuel injector for DISI engines under well-controlled turbulence conditions. It is not trivial to perform such informed experiments routinely in an optical DISI engine due to the multiplicity of flow variables which are difficult to both characterize and control. Knowledge of the interaction of the spray with any turbulent gas motion is critical for the prediction of any in-cylinder spray breakup, convection and evaporation. Specifically, the spray structure at the boundary can cause, and be influenced by, entrainment of the gaseous medium into which the spray is injected. If this gas carries its own motion, as is the case in in-cylinder flows, the interaction of the liquid and gas motions can affect greatly the boundary spray structures and hence the evaporation and mixing regimes. Therefore, gasoline was injected from a multi-hole injector into a gas body with well characterised turbulence of levels typically expected in engines (2–4 m/s) and a range of controlled levels of fuel/gas temperature and pressure (typically 20–120 °C and 0.5–5.0 bar). Images of the spray were captured by high-speed camera equipment using backlight shadowgraphy, Schlieren and planar Laser illumination to provide relevant comparisons. Such results are useful to engine designers and spray modellers because accurate simulation of spray break-up mechanisms from first principles is very challenging and only models of limited applicability currently exist, especially at high fuel temperature and low gas pressure conditions where significant alteration of the spray's nominal pattern can occur (nominal pattern: the spray pattern at 20 °C, 1.0 bar as dictated by the designed geometry and angles of the nozzle holes). Observations of the spray-turbulence interaction are further discussed in terms of the Stokes number. The latter was studied for a range of fuels with different properties. To the best of the authors' knowledge this is the first time that data on the effect of ambient turbulence are presented for a multi-hole injector of DISI engines at conditions relevant to both early intake stroke injection strategies for homogeneous mixture formation and late compression stroke strategies for stratified mixture engine operation.

EXPERIMENT APPARATUS AND PROCEDURE

INJECTOR

A multi-hole injector designed for vertical installation in close spacing arrangement with the spark plug of a DISI engine was used. The injector had six nozzle holes in an asymmetric arrangement with different angles with respect to the vertical axis. **Figure 1** shows a schematic of the injector and its spray plumes through two views. Plumes 1 and 6 have been designed to pass on either sides of the spark plug i.e. one at the intake side and the other at the exhaust side of the engine. More details about the injector geometry, nozzle-hole angles

and spray formation in a quiescent environment and in a running DISI engine can be found in previous studies by the current authors [7–16].

FUELS

Experiments for this work were carried out using a commercial grade gasoline (RON95 without oxygenates) and iso-octane. However, in the discussion and analysis of the results the properties of four other single-component fuels have also been considered: ethanol, n-butanol, iso-octane and n-pentane. A commercial grade European gasoline contains several hydrocarbons typically about 35–40% C5 or lower, similar levels of C6–C8 and the remainder C9–C10 hydrocarbon chains. Iso-octane is a single component of gasoline with boiling point temperature of 99 °C at 1.0 bar, while n-pentane, also a single component of gasoline, boils at 36.1 °C. Ethanol boils at 78.4 °C and n-butanol at 117 °C when at atmospheric pressure. The distillation curve of the gasoline used, along with other typical physical and chemical properties of all the fuels considered in the current study, have been published elsewhere and are not repeated here for brevity [15].

INJECTION VESSELS

A number of experiments on the effect of turbulence on spray development were carried out in a high-pressure fan-stirred vessel. The vessel consists of a spherical stainless steel pressure vessel with an internal diameter of 380 mm and orthogonal windows on the horizontal plane for spray and combustion imaging. The chamber has been designed to withstand peak pressures up to 100 bar and as such is suitable for the combustion of fuels. The vessel was fitted with three orthogonal pairs of quartz windows 100 mm thick and 150 mm in diameter. This configuration allowed excellent optical access to the central measurement volume of 150 mm diameter. Four fans internal to the chamber on a tetrahedral layout generate isotropic turbulence with near zero mean (bulk flow) velocities in the central volume of the vessel. Each fan is independently driven by an 8 kW variable speed induction motor. This allows for independent control of turbulence intensity and in-cylinder conditions. The internal flow characteristics of the bomb have been fully characterised by [22] who found that the turbulence intensity was a linear function of the fan speed. These calibration measurements also have revealed that within the optically accessible central volume of 150 mm in diameter, the turbulence was nearly isotropic with no significant mean velocity, and the turbulence RMS velocity was found to vary linearly with the fan speed. The longitudinal integral length scale was found from spatial correlation using two LDA probes, one at a fixed position and the other at a variable horizontal distance. From these measurements, the integral length scale was found to be nearly constant inside the central measurement volume. Specifically, it was 25 mm at low turbulence levels (u′<1 m/s) and 20 mm at all greater turbulence levels. The vessel was located at the University of Leeds and has previously been used for many experiments published in a large volume of literature, which also contain further descriptions of the vessel and its operation, e.g. [23].

The injector was fitted into a specially designed mount positioned at the centre of the chamber at an inclination of 19° to allow better visualisation of all pairs of plumes. A band heater was attached to the injector to heat up its body temperature, replicating in situ heating of injectors mounted in DISI engine heads. A thermocouple sensor provided feedback to a temperature controller which regulated the injector temperature as required by each experiment. The temperature measured was that of the injector body, as this

was the best possible arrangement in obtaining the fuel temperature using the available apparatus. As a result of this, each time the system was heated to a particular test temperature and the temperature was held constant for an hour, allowing enough heat-soak for a uniform distribution of temperature within the whole injector mount mass, before spray imaging was conducted. Therefore, in this paper, the term 'injector-body temperature' corresponds to the temperature reading of this thermocouple, i.e., the temperature of the injector as close to the injector tip as possible. Turbulence intensities were set to nominal values of 0 m/s, 2 m/s and 4 m/s (typical of in-cylinder flows at 1000–2000 RPM, e.g. see [20, 24, 25] for flowfield data in latest DISI engine geometries). For spray testing at quiescent gas conditions, i.e. for u′=0 m/s, in-chamber gas and injector body temperatures were fixed at 20 °C, 50 °C, 90 °C and 120 °C. The fuel injection pressure was fixed at 150 bar. Fuel injection was carried out at conditions representative of low-load and full-load early injection strategies for homogeneous mixture preparation (0.5 bar and 1.0 bar gas pressure), as well as for injection strategies representative of stratified charge preparation or under boosted operation (5.0 bar gas pressure). For u′=2–4 m/s, tests were carried out primarily at 120 °C with 0.5 bar and 5.0 bar gas pressure.

It needs to be highlighted here that one difference between typical in-cylinder conditions at the end of the compression stroke and the fan-stirred vessel is associated with dimensional scaling of the turbulent eddies, hence this vessel has been used extensively for studies of turbulent combustion relevant to conditions of early flame kernel development in spark-ignition engines, e.g. see [26, 27]. The integral length scale in the fan-stirred vessel was 20 mm for the conditions of interest (u′=2–4 m/s), hence the scale of these eddies in relation to the physical size of the spray and atomised droplets needs to be taken into account during the analysis. Furthermore, the Taylor scales in the vessel were of the order 0.3–0.5 mm for u′=2–4 m/s and the corresponding Kolmogorov scales about 6–10 μm [28]. For reference, in an engine, air flow turbulent eddies of integral size have been measured to be about 10%–20% of the clearance height [29], i.e. typically about 2–4 mm towards the end of compression or of the order 10–20 mm when the piston is close to BDC. Additionally structures of the order 2–3 mm in diameter have been typically observed throughout the intake stroke of the engine that the injector of the current study was originally designed for (when run at 1500 RPM) [20]; such eddies are considered to be between the Taylor and integral scales. Therefore, in an engine the length scales are generally smaller than in the fan-stirred vessel and perhaps more scaled to the physical dimensions of the spray and the facets of its break-up. However, the combination of turbulence intensities, eddy sizes and timescales in the vessel were still representative of a typical engine where macro structures of in-cylinder tumble' and 'swirl' are also present and where injection can occur into various degrees and scales of turbulence depending on injection strategy and engine load.

The sprays were also studied in the injection chambers of the fuel systems test facility of UCL at quiescent conditions with 20 °C gas temperature. Details about the chambers can be found in earlier studies by the current authors [11–15]. The fuel injection pressure was kept fixed at 150 bar and the effect of gas, i.e. 'back', pressure was studied in the range 0.5–5.0 bar. The injector was mounted at the top of the chamber in the same way to that used on the Leeds chamber and the injector body temperature was also varied from 20–120 °C using a band heater. Different imaging techniques were employed and compared at Leeds and UCL, as described in the next section.

SPRAY VISUALIZATION SETUP

Schlieren imaging of the spray was carried out in the fan-stirred vessel. In the Schlieren technique a light source is focused on the region of interest, where the light is diffracted by density gradients and hence these can be imaged by focusing the detected image on the camera lens. Hence, Schlieren images are sensitive to the first spatial derivative of light diffraction, and hence are much more sensitive to low refractive index gradients and suitable to the imaging of the vapour surrounding the liquid spray. The light for the Schlieren imaging was provided by a 20 W tungsten lamp and was directed along the horizontal axis of the vessel. Two identical plano-convex lenses, with a focal length of 1,000 mm, were used to produce parallel light beams of 150 mm through the visible central volume of the vessel. These were refracted during injection due to refractive index differences between the fuel vapor and nitrogen atmosphere and then, following previously published work and optimisation practices, focussed and directed toward a 0.65 mm pinhole placed in front of the camera, which captured the Schlieren images (a discussion on pinhole versus knife-edge selection can be found in [30]).

Mie Scattering as an imaging technique refers to the scatter of an incident light source by particles. In the case of spray imaging the light source is usually a laser sheet along the spray axis and the particles are the spray droplets. In this work, laser sheet illumination of the spray was carried out in the Leeds chamber using an Oxford LS 20 copper vapour laser synchronised to the camera frame rate. Specifically, the laser produced 15 ns pulses, each with 2 mJ and a wavelength of 510.6 nm. A series of mirrors and sheet forming optics aligned the beam vertically with the centre of the spray. The laser light was directed to the flow region of interest by three high-power transmitting mirrors and a laser sheet formed by first passing the beam through a spherical bi-convex lens with a 900 mm focal length that focused the beam through a cylindrical plano-convex lens with a focal length of 1,000 mm. The latter produced a laser sheet (measured to be of the order 0.5–1 mm thick) that passed through the vessel window and intersected with the fuel spray.

As a result of the geometry of the injector, each imaged spray plume was essentially the superposition of two plumes (see Z-Y view in **Figure 1**). Injection duration was held constant at 1.5 ms pulse-width for all conditions, with the camera recording for 2.5 ms each injection to capture initial, steady-state, end of injection and post injection spray characteristics. Due to obscuration of the spray tips by the pressure chamber windows, it was only possible to measure spray tip penetrations until approximately 1.0 ms After the Start Of Injection (ASOI, i.e. the time period following the rising edge of the trigger pulse sent to the injector driver unit). The average driver delay from the start of the injection pulse (Start of Injection, SOI) to fuel seen at the injector tip was of the order 300 μs, as has been quantified in detail in [12]. Triggering synchronisation was provided by an AVL 327 engine timing unit. 200 injection events and an average background image were captured. The background image for each time interval in the imaging sequence was removed from the spray images to account for differences in lighting over each run. Each corrected image was then thresholded at a value based on the mean of background pixels to leave a binary image. The image was then rotated to align each plume pair with the vertical axis and each plume pair was 'scanned' to find the plume tip. The distance from the plume tip to the nozzle was scaled to calculate a plume pair length. To determine the optimum threshold for automated processing, detailed sensitivity analysis was carried out on

the penetration based on different threshold levels and the uncertainty in the calculated values was found to be better than 4%.

Spray imaging was carried out using a pair of high speed CMOS cameras (Photron APX-RS and Phantom v4) at a frame rate of 10,000 frames per second, equivalent to one spray image per 0.9 degree Crank Angle (° CA) for an engine running at 1500 RPM. The cameras allowed a maximum resolution of 512×512 pixels at this frame rate and the optical arrangement corresponded to about 200 μm/pixel. The shutter was set to 1 μs. A mirror was placed at an angle of 45° to the imaging window to allow simultaneous recording (half-silvered). A dichroic filter, which blocked light at the laser wavelength of 510.6 nm, was placed over the lens of the Schlieren imaging camera to avoid saturation by the laser light during the simultaneous application of imaging techniques. The experimental arrangements were consistent with other studies of spray formation in the same vessel, such as those of Jakubik et al. [28] for a single-hole Diesel injector and Edabaway et al. [21] for a pressure-swirl atomizer. A schematic of the experimental arrangement is shown in **Figure 2**. The plane axes of **Figure 1** have also been included in **Figure 2** to clarify the views and planes of alignment. It is also reminded that the injector was rotated by 19° on plane Z-Y to allow better imaging of plume pair 1,6 (anticlockwise with respect to the vertical injector position shown in the Z-Y view of **Figure 1**; see also detailed drawing of injector mount in [11, 12] if required). Further information on how the positioning of the Laser sheet illuminated the plumes and emphasised the spray collapse form is provided in the results section.

Spray images were also acquired in the quiescent injection chamber of UCL using high-speed shadowgraphy with backlighting provided by a Multiblitz Variolite 500 flash gun diffused through a semi opaque Perspex board. Shadowgraphs respond to the second gradient of the refractive index and, here, capture the liquid phase of the spray. For these experiments the Photron APX-RS camera was run at frame rate of 9,000 per second at 640×480 pixels, corresponding to 1° CA for an engine running at 1500 PM. The optical arrangement corresponded to about 160 μm/pixel and the shutter was set to 1 μs. The injector was mounted on the chamber at the same inclination and orientation to that employed on the fan-stirred vessel. The fuel temperature was varied from 20–120 °C and the ambient pressure was set to 0.5 bar or 1 bar. The gas temperature in the chamber was not heated but was monitored and kept nominally at 20 °C. The experimental arrangement was consistent with previous studies of spray formation in the same injection chamber, such as those of [11–15] with the same multi-hole injector and a range of fuels, therefore, the reader is guided to these publications for more details on the chamber, experimental set-up, image processing techniques and uncertainties. These experiments were used to complement the work in the fan stirred vessel and observe phenomena at quiescent 20 °C conditions in comparison to those in the heated fan-stirred vessel. For a full discussion of the relative merits of the backlit imaging techniques of shadowraphy and Schlieren, optical set-ups and application the reader is guided to [30]. Mean and RMS images were calculated from 20 injection events recorded at each condition during the experiment.

RESULTS AND DISCUSSION

SPRAY DEVELOPMENT IN QUIESCENT CONDITIONS

Figure 3 and **Figure 4** show typical images of spray formation at quiescent ambient conditions using backlighting (shadowgraphy), Schlieren visualisation and Mie scattering (planar Laser illumination) for

gasoline and iso-octane fuels, respectively. It needs to be noted here that the set-up of the Mie scattering imaging system specifically enabled image saturation of the dense spray to visualize the spray border and the liquid structures in the spray mixing region of plume pairs 3,4 and 2,5 (see earlier **Figure 1** for numbering conventions). Plume pair 1,6 could not be analysed from the Leeds chamber images due to obscuration by the presence of a spark plug used for combustion studies in this chamber, as clearly seen in the Schlieren images of **Figures 3–4.** In the Mie images, the arrangement led to an intense image of the real spray at the centre of the chamber and a weaker 'ghost' image (below the real spray) that was a reflection from the back window; this did not affect the image processing method in the region of interest of the tips of the far right plume pairs 3,4 and 2,5. It is also noted that the separation between holes on the symmetry plane similar to the outer diameter of each hole (0.5 mm), hence the Laser-sheet, even at its thinnest waist of 0.5–1.0 mm did illuminate the edges of the spray especially closer to the nozzle hole exit either side of the symmetry plane.

Quantitative analysis on the full batch of processed images produced the spray penetration curves for each of the techniques at the baseline condition of 20 °C fuel temperature, 1.0 bar gas pressure as shown in **Figure 5** for gasoline and **Figure 6** for iso-octane. The values shown for all methods and conditions are the mean of the penetrations of plume pairs 3,4 and 2,5. In all cases the Schlieren (Leeds chamber) and backlit shadowgraph results (UCL chamber) match relatively closely. The Schlieren images produced slightly longer plume measurements on account of the imaging of the fuel vapour around the plume, as well as the actual liquid plume imaged by the shadowgraph technique. The Mie images show shorter penetration past about 800 μs ASOI; this is an effect of the illumination of the spray plumes solely on the vertical plane that did not allow light scattering by the fuel's droplets at the leading edge of the spray when the plumes had grown to size out of (i.e. through and in front of) that vertical plane.

Figures 7–8 show the effect of change in gas pressure (0.5 bar and 5.0 bar) and injector/gas temperature (90 °C and 120 °C) for gasoline. **Figure 9** and **Figure 11** show the respective effects for iso-octane, whilst **Figure 10** shows the pressure effect for iso-octane at 50 °C. In all cases, the Schlieren penetration is higher than those of Mie and backlighting. The only exception to this is for iso-octane at 90 °C and 120 °C in **Figure 10** and **Figure 11**, respectively, where the backlit images produced greater penetration. It needs to be highlighted that this is due to the gas in the Leeds chamber being that of the fuel temperature, whereas it was monitored at 20 °C for measurements carried out at UCL. Therefore, the effect shown is that of the increasing evaporation of the iso-octane spray at gas temperatures of 90–120 °C that reduced the imaged plume length.

For the Mie images captured with the vertical laser sheet across the central spray axis, the measured plume penetrations were typically shorter than for either the backlit shadowgraph or Schlieren technique, due to the sheet not illuminating the plumes once they have passed through the sheet. The exception to this is for the fully collapsed spray condition observed for gasoline at 120 °C, 0.5 bar gas pressure in **Figure 8**, where the collapsed plumes were drawn into the central axis of the spray, and hence into the laser sheet. This acted to increase the illuminated spray length, and hence the measured plume penetration was greatest for this condition. To highlight this and, for better direct comparison, **Figures 12–15** have grouped the spray penetrations for gasoline and iso-octane at all conditions for the Schlieren and Mie techniques separately.

The reduced penetration at 5.0 bar is clearly observed for all techniques at all conditions, as is the small effect of temperature on inducing smaller liquid penetration (Mie imaging) at this high pressure of 'uncollapsed' spray formation. It is also noted that in the Mie data of gasoline at 0.5 bar in **Figure 14**, the penetration increases gradually as the spray is gradually changing formation shape from its nominal 6-plume pattern to that of a large collapsed plume moving faster vertically down and getting aligned with the centre of the chamber, i.e. drawn back on the illumination plane of the Laser. For iso-octane, the respective Mie data of 0.5 bar in **Figure 15** demonstrate that the spray's penetration reduces as faster evaporation is engaged but no spray collapse is induced. The effect is also clear in the simultaneously acquired Schlieren data of **Figure 13**, where the faster evaporation and dispersion of vapour led to decreased imaged penetration at higher temperatures.

SPRAY DEVELOPMENT IN TURBULENCE

Typical, mean and RMS spray images for each condition are shown at 0.5 and 5.0 bar in **Figure 16** and **Figure 17**, respectively, using the Schlieren imaging technique, which is sensitive to both the liquid and vapour phases of the fuel. These show clearly that at the lower gas pressure of 0.5 bar in **Figure 16** the effect of the turbulent air motion results in significantly increased dispersion of the spray in comparison to 5.0 bar in **Figure 17**. The volume of visible spray is much smaller than for the same changes in turbulence level at the higher gas pressure of 5.0 bar in **Figure 17**. The liquid has broken up and presumably further evaporated as small-scale mixing with the ambient gas is faster, bringing, in turn, the mixture to equilibrium faster. The gradients are then too fine to be detected by the sensitivity of the Schlieren system (still diffracting light, though). Those images may be compared to observations from the same chamber and with the same Schlieren system using a single-plume Diesel spray in [28]. In that work the outer spray envelope of the Schlieren image was seen to elongate with increasing levels of turbulence, whilst the internal liquid core reduced slightly in length. This led to the conclusion that increasing the magnitude of turbulence intensity resulted in an increased rate of evaporation of the Diesel fuel. A similar mechanism is seen in the results presented in the current paper but the higher volatility of gasoline in comparison to Diesel leads to more rapid evaporation of the gasoline fuel with increasing turbulence so that no vapour may be detected, leading to an overall reduction in the dense spray length for $u'=2$–4 m/s. The loss of liquid and detectable vapour gradients at the low gas pressure from the rapid rate of vaporisation for this condition can be favourably analogous to those required in an engine for early injection strategies where the desire is to create a fully mixed, homogeneously dispersed air/fuel charge throughout the entire combustion chamber. Likewise, for later injection into a high pressure atmosphere (i.e. during the compression stroke prior to ignition), the desire is to create a highly stable, localised air/fuel charge around the spark plug which is not influenced by the turbulent flow structures; however, penetration should be such as not to hit directly the piston crown and/or or cylinder walls. This means that short injection durations are favourable at these conditions. If the spray had to be dispersed solely by turbulence then levels much higher than the typically present in-cylinder values of $u'=2$–4 m/s (at 1500 RPM) would be needed.

The mean and RMS images in **Figures 16–17** also demonstrate the effect of turbulence on the spray envelope variability. In these images, high variability is shown by white pixels with reducing greyscale tones

to black representing no variability in tonal value over the different images. Specifically, the RMS images of 0.5 bar in **Figure 16** show an increase in the width of the variability region around the spray at a turbulence intensity of 2 m/s relative to the quiescent condition of 0 m/s, especially at the spray plume tips. However, at u'=4 m/s the width of variation around the core of the spray is greatly reduced. This highlights a shorter and 'more repeatable' imaged dense core (within the sensitivity of the current Schlieren arrangement), since atomisation and mixing on the periphery of the core is greatly enhanced at this high degree of turbulence. At the high gas pressure condition of 5.0 bar though, a similar level of variability is evident at all levels of turbulence in **Figure 17**. If the effect of the turbulent air motion in entraining the droplets and vapour at the spray tip and boundary are considered, a trend in these variability observations seems to emerge. Specifically, it may be argued that at a gas pressure of 0.5 bar, the fuel droplets produced by aerodynamic break-up at and near the spray plume leading edge are entrained and clustered at a turbulence intensity of 2 m/s, reducing their localised vaporisation rate. Thereby the droplet residence time is increased and, allied to the 'random' turbulent air motion, the variability is increased. At a turbulence intensity of 4 m/s the droplets are entrained but the higher turbulent energy can lead to an increase in secondary break-up, and hence these smaller droplets are either fully vaporised or any remaining small droplets are not clustered but swept away from the spray boundary. The repeatability of this effect and reduction in clustering leads to a reduced variability in spray boundary location at these conditions. At a gas pressure of 1.0 bar the droplet sizes have been measured to be larger than at 0.5 bar with this injector [15] and at 5.0 bar they are expected to be even larger on the basis of work with other multi-hole injectors [31] and typical textbooks [32, 33], hence the probability of their entrainment into clusters is reduced, and so similar levels of variability are detected for all turbulence conditions; although at a turbulence intensity of 4 m/s some entrainment occurs and hence a slightly higher level of variability is actually detected. It is noted here that further work is required to clarify the details of such a potential mechanism, particularly with higher magnification imaging and droplet sizing.

The effect of gas turbulence on the spray's formation has been quantified in terms of spray area and plume penetration in **Figures 18–21** for 0.5 bar and 5.0 bar gas pressure. The shorter plume lengths at the high gas pressure condition of 5.0 bar than at the low gas pressure of 0.5 bar are evident. The differences in plume penetration or imaged spray area at 5.0 bar over the range of turbulence intensities 0–4 m/s are marginal, albeit consistent between the Schlieren and Mie data. The backlit data show a much smaller spray area at quiescent conditions than the Schlieren data due to the entire gas body being at the same temperature as the injector in the Leeds chamber (i.e. 120 °C), whereas the gas body in the quiescent chamber at UCL was monitored to be nominally at 20 °C. The effect of that was the presence of clearly wider plumes recorded by the Schlieren arrangement due to the large amount of vapour around the liquid core.

The increase in plume penetration due to the effect of decreasing pressure between the 5.0 bar and 0.5 bar gas pressure conditions is approximately 15–20% at quiescent conditions. The spray area is dramatically smaller at about 1 ms ASOI by about 70% for 4 m/s in comparison to that of 0 m/s. The respective effect on penetration is about 40–50% for both Schlieren and Mie data. In fact, the recorded penetration at 0.5 bar for u'=4 m/s is lower than the penetration of the spray at 5.0 bar. This reduction can be a key consideration for in-cylinder mixing. For better clarity it may be noted that the Schlieren technique images refractive index

gradients around the liquid which result from fuel vaporisation and hence fully vaporised fuel is not depicted. Therefore, the Schlieren images are not a measurement of the total volume of fuel vaporised but may be used to indicate regions where vaporisation occurs, and the volume of partially vaporised fuel present around the spray periphery. To capture any smaller refractive index gradients, one would need a much longer Schlieren system and this was not considered essential within the objectives of the current work.

DROPLET INTERACTION WITH TURBULENT GAS MOTION

For general spray characterisation of the distribution of droplets in low droplet concentration density sprays, where creeping flow could be assumed to exist around the individual droplets, and large scales of turbulence are reported to affect the spray structure, the use of the Stokes number has been found well suited to the qualitative indication of the likelihood of droplets around a spray being convected by the surrounding gas turbulence [34]. The Stokes number can be mathematically expressed by:

$$\text{St} = \frac{\tau_D}{\tau_L}$$

where τ_D is the droplet response time and τ_L is the integral time-scale of the turbulence. The Stokes number can also be defined with respect to other scales of turbulence, typically the Taylor (τ_λ) or the Kolmogorov (τ_k) time-scale. Using the droplet's equation of motion, the droplet response time τ_D is given by [35]):

$$\tau_D = \frac{4D\rho_L}{3C_D\rho_g u}$$

where D is the droplet diameter, ρ_L is the droplet density, C_D is the coefficient of drag, ρ_g is the gas density and u is the relative droplet velocity. For spherical particle Reynolds numbers much lower than one (typically lower than about 0.01), C_D can be calculated by Stokes's law as 24/Re, whilst for Re greater than 0.01, C_D can be calculated by applying a correction to Stokes's law as $(24/\text{Re})(1+0.15\text{Re}^{0.687})$ [36, 37]. Alternatively, for Reynolds numbers lower than 1000, C_D can be calculated by $(24/\text{Re})(1+\text{Re}^{2/3}/6)$ and fixed to 0.424 for Reynolds numbers lower than that [28]. Based on the ratio of the droplet and gas turbulence response times, if St<<1 the droplet is likely to be captured in the turbulent eddy and follow the eddy's motion. Conversely, a high turbulent velocity gives short turbulent time scale and hence leads to an increase in Stokes number. In the extreme case, a droplet does not have time to react to rapid changes in the turbulent air flow, and so if St>>1 the droplet trajectory is notionally unaffected by the turbulent motion. At St~1 the droplet is centrifuged towards the outer edge of the eddy, and the droplet trajectory is both vortical and perpendicular to that of the eddy, and the droplet spirals through the vortex. Beard et al. [38] reported a strong dependency of individual droplet trajectories on large scale vortex dynamics and Wark et al. [39] confirmed the presence of droplet clusters at the spray boundary and their dependence on the air flow turbulence. Sornek et al. [34] reported a considerable qualitative change in the size and spatial distribution of the droplet clusters that were present inside the spray under different turbulence conditions. They also quantified the droplet-turbulence interactions by means of the centrifugal Stokes number which is a measure of the turbulent vortex centrifugal force relative to the droplet drag force, and as such is another measure of the likelihood of droplet entrainment into the turbulent flow structure and subsequent vaporisation. They obtained values in the range of 0.1 to 1 for the centrifugal Stokes number. At the lower limit, they reported

nearly homogeneous droplet dispersion, whilst with increasing Stokes number the droplets tended to form droplet clusters of increasing size at the outer edge of the turbulent eddies. According to their findings, the mechanism of droplet clustering may exist up to higher limits of St~10, at which point dense clusters can result in non-transparent regions observable by optical techniques. Moreover, they also found that in these dense droplet clusters, the rate of vaporisation was reduced due to the near-droplet interactions.

However, specifically for dense sprays such as those relevant to DISI engines, some of the aforementioned assumptions are no longer strictly valid and the estimation of the Stokes number becomes harder. Dan et al. [40] identified the motion of the entrained air as the probable mechanism for the establishment of coherent liquid structures, determined to be dense clusters of droplets, around the periphery of Diesel spray plumes. The authors also stated that their spatial distribution can be described by means of the aerodynamic response to the range of turbulent vortices present inside the spray. In relation to vaporising Diesel sprays, Siebers [41, 42] concluded that the rate of vaporisation is controlled by the air entrainment and turbulent mixing of the liquid and gaseous phases. The vaporisation rate of the droplets, which is directly influenced by the local droplet concentration density, may be indicated by the Stokes number for these situations.

Although Dan et al. [40] has suggested that the Stokes number is also valid in Diesel-like sprays, it is probable that the high droplet concentration density of such direct injection sprays alter the interaction between the turbulence and the fuel spray, limiting the validity of a typical Stokes number analysis, especially in the absence of relevant high-resolution quantitative data. Some later imaging data also with Diesel sprays suggested that the Stokes relationship also held for such dense droplet fields, albeit acting possibly at lower Stokes numbers than those which the relationship is usually associated with [28]. Additionally, although the relationship between spray break-up and Stokes number was originally developed for low volatility sprays, where significant evaporation which could influence that of the adjacent droplets was not present, some data with an air jet laden by high volatility fuel droplets have shown that the relationship could still be valid [39]. Therefore, in the absence of a more accurate assessment of the interaction of the gas motion and spray boundary, an estimation of Stokes numbers derived from measured quantities of droplet sizes and velocities over a range of fuel types relevant to spark-ignition engines was considered potentially informative. Our previously published work with this injector at quiescent chamber conditions focused on analysis of the Weber and Ohnesorge numbers. An attempt to calculate Stokes numbers relevant to the same injector under study here and the turbulent time scales in the fan-stirred vessel is discussed henceforward using data available from this and previously published work.

Droplet sizing for the same injector with iso-octane, gasoline and n-pentane fuels has been performed by Phase Doppler Anemometry (PDA) under quiescent conditions over a range of conditions and published in [15]. The initial ensemble-averaged droplet diameter for gasoline at 20 °C, 1 bar was ~15 µm and was seen to reduce over the injection to ~11 µm; however, individual droplets as large as 30 µm and as small as 2 µm were captured. The droplets at the leading edge of n-pentane were slightly smaller than gasoline's and iso-octane's (~13 µm). The mid-injection average droplet size was also slightly lower for n-pentane than for the other fuels (~10 µm), potentially a result of n-pentane's higher volatility and lower viscosity. The Sauter Mean Diameter (SMD) illustrated critical differences between gasoline, iso-octane and n-pentane in the

behaviour of droplet reduction with temperature/pressure when moving from uncollapsed to collapsed spray conditions. Specifically, at 20 °C, 1.0 bar, the SMD was ~15–17 µm for all fuels and for gasoline and n-pentane, increasing the injector body temperature steadily decreased the SMD. In contrast, iso-octane's SMD showed only little variation with increasing temperature until 120 °C was approached. The rapid reduction in SMD at 120 °C and beyond at 0.5 bar suggested that the rate of break-up and/or vaporisation had increased greatly once the boiling point of iso-octane had been exceeded. Initial spray plume convergence appeared when the SMD fell below ~12 µm. This suggested that such a size led to diminished droplet momentum along the spray's plume trajectory to the extent that droplets were drawn into the central spray region and this migration acted to pull the plumes together into a 'collapsed' form. Ethanol and n-butanol droplet sizes from multi-hole injectors have been obtained by [43] and showed that ethanol had about 30–40% larger SMD than gasoline, whilst n-butanol about 40–50% larger, over the range of conditions considered here. Relevant droplet velocities within the spray have been quantified by a combination of PDA measurements and spray tip penetration curves from high-speed imaging [11, 12, 15]. Specifically, once the spray had penetrated past 20 mm from the nozzle tip, these velocities were typically in the range 30–90 m/s under quiescent conditions. It is noted that the gradient of the penetration curves of Figure 20 at 5.0 bar in the range 0.7–1.1 ms ASOI was found to be about 30–40 m/s for all values of turbulent intensity, whilst from Figure 21 gradients of about 30–60 m/s were calculated for decreasing levels of turbulence from 4 to 0 m/s. For the purpose of the current exercise in estimating Stokes numbers, droplet velocities were set to half the values within the dense spray quoted above, as this approach was considered an informed compromise of what is happening between the core and the periphery of the spray (i.e. no very fast droplets or droplets that had already slowed down to levels of the ambient turbulent intensity).

The calculated Stokes numbers are shown graphically in **Figure 22** for the integral and Taylor scales[1]. The integral scale Stokes exhibits values considerably lower than 1, suggesting that the droplets for all conditions would be likely entrained into the turbulent vortices. However, the previous assessment of the RMS spray images would suggest that this was not necessarily case, and that entrainment and clustering for gasoline was present on a large scale mainly at 0.5 bar gas pressure and u′=2 m/s. Stokes number with similar values to those calculated in the current work have been obtained for a single plume Diesel spray by [28]. Specifically the latter authors calculated that increasing the ambient turbulence from 2 m/s to 4 m/s led to an increase in the integral scale Stokes number from 0.005 to 0.02. This was manifest by increased droplet clustering in the mixing region of the Diesel spray, mainly indicated by an increased size of the liquid structures and decreasing distance between them. An assessment of the Stokes number in relation to the gasoline sprays studied here shows that whilst an increased level of turbulence would be expected to lead to a reduction in vaporisation, the large scale eddies actually worked to carry dense fuel vapour away from the spray by

---

[1]A constraint of the Stokes number analysis is that the droplets should not be larger than the size of the turbulent eddies, otherwise assumptions of possible droplet centrifugal motion in the eddy would not be valid. Such assumptions were valid for the integral and Taylor scales but invalid for the Kolmogorov scales since some measured droplets were smaller than the Kolmogorov scale and such droplets would modulate the turbulence. This matter merits further work, hence only integral and Taylor Stokes numbers are presented in this paper.

enhancing the mixing process. Hence the vaporisation rate was found to increase with an increase in turbulence intensity.

The current results obtained with higher volatility fuel sprays than the previously studied Diesel sprays, and with dense droplet and vapour regions around the spray boundary, also show differences in the Stokes numbers over which droplets are conveyed away from the spray, over which clusters are formed and over which sprays may be minimally affected. These ranges appear again not to be centred on a Stokes number value of 1, but on a lower potentially 'critical' Stokes number, at which clustering is most likely to occur. From the resolution of experimental data points in this work, the critical integral scale Stokes number appears to fall in the range 0.005–0.01 for gasoline, whilst for Diesel fuel values of 0.02–0.03 have been reported in [28]. The respective Taylor scale Stokes number lies in a region of about 0.1. When considering the spray images discussed earlier, it may be hypothesised that a representative function of the drop clustering probability with respect to integral Stokes number may possibly exhibit some form of 'peak' in the area of critical Stokes. Investigation into the potential shape of such a relationship was well outside the immediate objectives of the current work but it could add significant value to the still limited state of knowledge on the interaction between the spray's development and the in-cylinder air motion that is particularly important for the robust operation of a direct injection spark ignition engine over a range of operating conditions and fuel types.

Although only gasoline was tested in the fan-stirred chamber with turbulent gas motion, Stokes numbers were also estimated for iso-octane (whose boiling point is located in the middle region of a typical gasoline's distillation curve), n-pentane (that represents the very high volatility components of a typical gasoline that drive the mechanism of spray collapse), as well as the common alcohols ethanol and n-butanol. This was done to enable an analysis of the effect of fuel properties on break-up and mixing in turbulent flows in comparison to the trends observed for gasoline. Properties of all those fuels over a range of conditions were obtained from [44]. The integral Stokes number was calculated for each fuel over the tested injector body temperature range of 20–120 °C as shown in **Figures 23–25** for u′=2–4 m/s. The graphs show, typically, a decrease in the Stokes number with an increase in temperature, principally due to a decrease in droplet size and liquid density. Gasoline and iso-octane are closely matched, with n-pentane residing clearly lower on the charts. The alcohols exhibit larger Stokes than the hydrocarbons over the full temperature range. Based on a critical Stokes number of about 0.005–0.01, at lower temperatures the larger droplets would be expected to remain generally unaffected by the turbulent gas motion, although any fuel vapour (which would be low for most of these fuels at such conditions) would be entrained by the air motion and hence both variability in the spatial distribution of the fuel and the effect on plume penetration would be weak. With increasing fuel temperature, the effects of both of these mechanisms are expected to increase primarily in line with the fuel's volatility, suggesting that the balance between volatility and density is a key indicator of the fuel's likely susceptibility to the influence of turbulence on its spray break-up and mixing. For the alcohols, the effect of viscosity is critical, as it can dominate the mechanism of atomization and resultant droplet sizes, hence the values of the Stokes number were larger over the range of temperature shown.

At the Taylor scale, the respective Stokes numbers in **Figures 26–28** increase to values of the order 1 for the alcohols, particularly at the lower temperatures with increasing ambient turbulence. Considering that droplet sizes were of the same order as the Kolmogorov length scale in the fan-stirred vessel, the predominant scale for droplet clustering was the Taylor scale. If it is also considered that the Taylor scale was just about 1.5–2.5 times the pixel resolution at u′=2–4 m/s and that wide grayscale distinction was observed between structures within the collapsed spray at u′=2 m/s and narrower at all other conditions, then the mechanisms described above are generally supported by the experimental observations. However, it is iterated here that all the aforementioned values of Stokes were calculated as simple means to discuss the effect of fuel volatility, thermodynamic conditions and turbulence, within the resolution of the conducted tests, therefore, further work is required to provide more solid arguments and to understand the practical effect of the relatively small differences observed between fuels. It is hypothesized that the representation of fuel spray droplets and gas interactions through an improved indicator that, apart from the Stokes number, may also include other metrics like the Weber and Ohnesorge numbers could allow for a more precise analysis and prediction of the conditions under which turbulence strongly influences the spray break-up and evaporation rate for a variety of fuel types.

SUMMARY AND CONCLUSIONS

This paper presented a study into the effect of ambient turbulence and thermodynamic conditions on fuel spray formation for a multi-hole injector for DISI engines. Gasoline and iso-octane fuels were employed over a range of fuel temperatures (20–120 °C), ambient temperatures (20–120 °C) and pressures (0.5–5.0 bar). Shadowgraphy, Schlieren and planar Laser illumination spray imaging techniques were used. The results illustrated that the interaction of the fuel spray and gas body plays an important role in the spray's development particularly at conditions of fuel flash boiling. The turbulent gas motion acts to affect the concentration of droplets and fuel vapour at the spray's periphery, which in turn affect the local vaporisation rate through limiting the local concentration gradient. This alters the physical spray form in terms of penetration length and dense liquid spray area. The effect of turbulence on the spray's development at non-flash boiling thermodynamic conditions is much weaker. The main conclusions of this work can be summarised as follows:

- Over a range 20–120 °C and 0.5–5.0 bar, the Schlieren penetration was higher than that of Mie and backlighting. The only exception was iso-octane at 90 °C and 120 °C where the backlit images produced greater penetration. This was due to the gas in the Schlieren chamber being that of the fuel temperature, whereas it was 20 °C for the backlit work, i.e. increasing evaporation at gas temperatures of 90–120 °C reduced the imaged plume length.

- For the Mie images, the measured plume penetrations were shorter than either the backlit or Schlieren technique, due to the sheet not illuminating the plumes once they have passed through the vertical sheet. The exception to this was the fully collapsed gasoline spray at 120 °C, 0.5 bar gas pressure, where the collapsed plumes were drawn into the central axis of the spray, and hence into the laser sheet. Hence the measured plume penetration was greatest for this condition and very close to the Schlieren penetration.

- Reduced penetration was clearly observed at 5.0 bar in comparison to 0.5 bar and 1.0 bar, with a weak effect of temperature on inducing shorter penetration at this 'uncollapsed' spray formation. In the Mie data of gasoline at 0.5 bar the penetration increased gradually as the spray gradually changed formation pattern from the nominal one to that of a large collapsed plume moving faster vertically and getting aligned with the centre of the chamber, i.e. drawn back on the illumination plane of the Laser. For iso-octane, the Mie data of 0.5 bar showed that the spray's penetration reduced as faster evaporation was engaged despite the absence of spray collapse. The effect was also present in the Schlieren data, where the faster evaporation and dispersion of vapour led to lower penetration at higher temperatures.

- At 0.5 bar gas pressure, the effect of increased turbulent intensity u′ was a significantly increased dispersion of the spray. The volume of visible spray at higher u′ was much smaller than for the same changes in turbulence level at 5.0 bar.

- The spray images at 0.5 bar showed an increase in the width of the high RMS region around the spray at u′=2 m/s relative to u′=0 m/s, especially at the spray plume tip. At u′=4 m/s the width of RMS around the core of the spray was greatly reduced. This suggested that at 0.5 bar, the droplets near the spray plume were entrained and potentially clustered at a turbulence intensity of 2 m/s, reducing their localised evaporation rate. Thereby the droplet residence time increased and, allied to the 'random' turbulent air motion, the RMS in the detected regions increased. At u′=4 m/s, the droplets were entrained but the higher turbulent energy swept them away from the spray boundary by enhanced mixing. The consistent repeatability of this effect from injection to injection was demonstrated by the reduced width of RMS at the spray boundary and was presumably associated with a reduction in clustering regions. At a gas pressure of 5.0 bar, the droplet sizes were greater and hence the probability of their entrainment into clusters reduced, hence similar levels and regions of RMS were found for all turbulence levels.

- At 5.0 bat, the differences in penetration or projected spray area over u′=0–4 m/s were marginal and consistent between Schlieren and Mie data. The increase in plume penetration due to the effect of decreasing pressure between the 5.0 bar and 0.5 bar gas pressure conditions was approximately 15–20% at u′=0 m/s. The spray area was smaller at about 1 ms ASOI by about 70% for u′=4 m/s in comparison to 0 m/s. The respective effect on penetration was 40–50% for both Schlieren and Mie data. The penetration at 0.5 bar for u′=4 m/s was even lower than the penetration at 5.0 bar. This reduction can be a key consideration for in-cylinder mixing and wall impingement phenomena.

- The integral scale Stokes number was found to be considerably lower than 1, suggesting that the droplets for all conditions would be likely entrained into the turbulent eddies. However, the assessment of the trends observed from the spray images would suggest that this was not case, and that entrainment and clustering was present primarily at 0.5 bar gas pressure and u′=2 m/s. An assessment of the Stokes number in relation to the spray suggested that whilst an increased u′ would be expected to lead to a reduction in vaporisation, the large scale turbulent eddies actually worked to carry dense fuel vapour away from the spray by enhanced mixing. Hence the dispersion and evaporation rate increased with an increase in u′.

- The results showed certain differences in the range of integral scale Stokes number over which droplets are conveyed away from the spray, over which clusters are formed and over which they are unaffected. These appeared not to be centred at a Stokes number strictly of the order 1 but on a lower critical Stokes number at which clustering was most likely to occur (typically in the range 0.005–0.01), presumably with some form of 'peaked' relationship at that point on a probability curve of droplet clustering versus Stokes.

- The effect of fuel properties on the integral and Taylor scale Stokes numbers was also examined by considering iso-octane, n-pentane, ethanol and n-butanol fuels. The results showed a decrease in Stokes with an increase in temperature for all fuels, principally due to decreased droplet sizes. Gasoline and iso-octane were closely-matched, n-pentane exhibited the lowest Stokes, whilst the alcohols generally the highest, reaching values of Stokes at the Taylor scale at 20 °C of the order 1.

- Based on the critical integral scale Stokes number, at lower temperatures the larger droplets would be expected to remain relatively unaffected by the turbulent gas motion for most fuels, although any fuel vapour (which would be low for most fuels tested at this condition) would be entrained and hence the RMS in spatial distribution of the fuel and the effect on plume penetration would be low. At higher temperatures the effect of fuel properties forced different fuels over or under the critical Stokes and the area of clustering around the spray would be expected to change accordingly depending on the level of turbulence intensity.

Further higher resolution optical studies are necessary to provide stronger quantitative analysis of the aforementioned phenomena and discussion on the Stokes number at which droplet clustering is most likely to occur for sprays relevant to DISI engines. The representation of spray/turbulence interactions through a further developed indicator that could include the Stokes number in conjunction with metrics like the Weber and Ohnesorge numbers could allow for a better analysis and prediction of those conditions under which turbulence strongly influences the spray break-up and subsequent evaporation for a range of fuels with diverse properties and volatilities.

REFERENCES

1. F. Zhao, M.C. Lai, D.L. Harrington, Automotive spark-ignition direct-injection gasoline engines, Progress in Energy and Combustion Science, Vol. 25, pp. 437–562, 1999.
2. Williams, P.A., O'Donaghue, S., Anderson, R.W. and Richardson, S.H., "An Experimental Study of the Spray Characteristics of Pressure-Swirl Atomisers for DISI Combustion Systems", SAE Paper 2001-01-1974, 2001.

3. Jashdan, J.T., Shrimpton, J.S. and Acroumanis, C., "Dynamic Structure of Direct Injection Gasoline Engine Sprays: Air Flow and Density Effects", Atomisation and Sprays, Vol. 12, pp. 539–557, 2002.

4. Araneo, L., Coghe, A., Brunello, G. and Donde, R., "Effects of Fuel Temperature and Ambient Pressure on a GDI Swirled Injector Spray", SAE Paper 2000-01-1901, 2000.

5. van der Wege B.A. and Hochgreb, S., "Effects of Fuel Volatility and Operating Conditions on Fuel Sprays in DISI Engines: (1) Imaging Investigation," SAE Paper 2000-01-0535, 2000.

6. T. Stach, J. Schlerfer, M. Vorbach, New generation multi-hole injector for direct-injection SI engines, SAE Paper 2007-01-1404, 2007.

7. J. Serras-Pereira, P.G. Aleiferis, D. Richardson, S. Wallace, Mixture formation and combustion variability in a spray-guided DISI engine, SAE Transactions, Journal of Engines, Vol. 116, pp. 1332–1356, SAE Paper 2007-01-4033, 2007.

8. J. Serras-Pereira, P.G. Aleiferis, D. Richardson, S. Wallace, Spray development, flow interactions and wall impingement in a DISI engine, SAE Paper 2007-01-2712, 2007.

9. Serras-Pereira, J., Aleiferis, P. G., Richardson, D., Wallace, S., "Characteristics of ethanol, butanol, Iso-octane and gasoline Sprays and Combustion from a Multi-Hole Injector in a DISI Engine", SAE International Journal of Fuels and Lubricants, Vol. 1, pp. 893–909, SAE Paper 2008-01-1591, 2008.

10. Serras-Pereira, J., Aleiferis, P. G., and Richardson, D., "An Analysis of the Combustion Behaviour of Ethanol, Butanol, Iso-Octane, Gasoline and Methane in a Direct-Injection Spark-Ignition Research Engine", Combustion Science and Technology, Vol 185, pp. 484–513, 2013.

11. van Romunde, Z., Aleiferis, P.G., Cracknell, R.F. and Walmsley, H.L., "Effect of Fuel Properties on Spray Development from a Multi-Hole DISI Engine Injector", SAE Transactions, Journal of Engines, Vol. 116, pp. 1313–1331, SAE Paper 2007-01-4032, 2007.

12. van Romunde, Z. and Aleiferis, P.G., "Effect of Operating Conditions and Fuel Volatility on Development and Variability of Sprays from gasoline Direct-Injection Multi-Hole Injectors" Atomization and Sprays, Vol. 19, pp. 207–234, 2009.

13. J. Serras-Pereira, Z. van Romunde, P.G. Aleiferis, D. Richardson, S. Wallace, R.F. Cracknell, "Cavitation, primary break-up and flash boiling of gasoline, iso-octane and n-pentane with a real-size optical direct-injection nozzle", Fuel, Vol. 89, pp. 2592–2607, 2010.

14. Aleiferis, P.G., Serras-Pereira, J., Augoye, A., Davies, T.J., Cracknell, R.F. and Richardson, D., "Effect of Fuel Temperature on In-Nozzle Cavitation and Spray Formation of Liquid Hydrocarbons and Alcohols from a Real-Size Optical Injector for Direct-Injection Spark-Ignition Engines", International Journal of Heat and Mass Transfer, Vol. 53, pp. 4588–4606, 2010.

15. Aleiferis, P. G. and van Romunde, Z., "An Analysis of Spray Development with Ethanol, Butanol, iso-Octane, n-Pentane and Gasoline Fuels from a Multi-Hole Injector under Hot Fuel Conditions", Fuel, Vol. 105, pp. 143–168, 2013.

16. Aleiferis, P.G., Serras-Pereira, J. and Richardson, D., "Imaging and Heat Flux Measurements of Impinging Sprays of Liquid Hydrocarbons and Alcohols in a Motoring and Firing Direct-Injection Spark-Ignition Engine", Fuel, Vol. 91, pp. 264–297, 2011.

17. Jarvis, S., Justham, T., Clarke, A., Garner, C.P., Hargrave, G.K. and Richardson, D., "Motored SI IC Engine In-Cylinder Flow Field Measurement Using time Resolved Digital PIV for Characterisation of Cyclic Variation", SAE Paper 2006-01-1044, 2006.

18. Bradley D., Haq M.Z., Hicks R.A., Kitagawa T., Lawes M., Sheppard C.G.W., Woolley R., "Turbulent Burning Velocity, burned Gas Distribution and Associated Flame Surface Definition", Combustion and Flame, Vol. 133, pp. 415–430, 2003.

19. Pajot, O., Mounaim-Rousselle, C., Queiros-Conde, D., "New Data on Flame Behaviour in Lean Burn S.I. Engine" SAE Paper 2001-01-1956, 2001.

20. Rimmer, J.E.T., Long, E.J., Garner, C.P., Hargrave, G.K., Richardson, D., Wallace, S., "The Influence of Single and Multiple Injection Strategies on In-Cylinder Flow and Combustion within a DISI Engine", SAE Paper 2009-01-0660, 2009.

21. Elbadawy, I., Gaskell, P.H., Lawes, M. and Thompson, H.M., "The Effects of Initial Ambient Turbulence Levels on Iso-octane Injection Sprays", Atomization and Sprays, Vol. 21, pp. 799–817, 2011.

22. Nwagwe I.K., Weller H.G., Tabor G.R., Gosman A.D., Lawes M., Sheppard C.W.G., Woolley R., "Measurements and Large Eddy Simulations of Turbulent Premixed Flame Kernel Growth", Proceedings of the Combustion Institute, Vol. 28, pp 59–65, 2000.

23. Bradley, D., Hicks, M., Lawes, M., Sheppard, C.G.W. and Woolley, R., "The Measurement of Laminar Burning Velocities and Markstein Numbers for iso-Octane–Air and iso-Octane–n-Heptane–Air Mixtures at Elevated Temperatures and Pressures in an Explosion Bomb", Combustion and Flame, Vol. 115, pp. 126–144, 1999.

24. Stansfield, P., Wigley, G., Catto, J. and Pitcher, G., "PIV Analysis of In-Cylinder Flow Structures over a Range of Realistic Engine Speeds", 13th Int Symp on Applications of Laser Techniques to Fluid Mechanics, Lisbon, Portugal, 26–29 June, 2006.

25. Malcolm, J.S., Behringer, M.K., Aleiferis, P.G., Mitcalf, J. and OudeNijeweme, D., "Characterisation of Flow Structures in a Direct-Injection Spark-Ignition Engine Using PIV, LDV and CFD", SAE Paper 2011-01-1290, 2011.

26. Lawes, M., Ormsby, M.P., Sheppard, C.G.W. and Woolley, R., "Variation of Turbulent Burning Rate of Methane, Methanol, and iso-Octane Air Mixtures with Equivalence Ratio at Elevated Pressure", Combustion Science and Technology, Vol. 177, pp. 1273–1289, 2005.

27. Bradley, D., Lawes, M. and Mansour, M.S., "Correlation of Turbulent Burning Velocities of Ethanol-Air, Measured in a Fan-Stirred Bomb up to 1.2 MPa", Combustion and Flame, Vol. 158, pp. 123–138, 2011.

28. Jakubik T, Lawes M., Woolley R., Jicha M., "Study of Ambient Turbulence Effects on Diesel Sprays in a Fan-Stirred Vessel", Atomization and Sprays, Vol. 16, pp. 687–703, 2006.

29. Fraser, R.A. and Bracco, F.V., "Cycle-resolved LDV integral length scale measurements in an IC engine", SAE Paper 880381, 1988.

30. Settles G.S., (2006), "Schlieren and Shadowgraph Techniques", Springer Verlag, Berlin.

31. Mitroglou, N., Nouri, J. M., Yan, Y., Gavaises, M. and Arcoumanis, C., "Spray Structure Generated by Multi-hole Injectors for Gasoline Direct-Injection Engines" SAE Paper 2007-01-1417, 2007.

32. Baumgarten, C., "Mixture Formation in Internal Combustion Engines", Springer, 2003.

33. Lefebvre, A., "Atomization and Sprays", CRC Press, 1988.

34. Sornek R.J., Dobashi R., Hirano T., "Effect of Turbulence on Vaporisation, Mixing and Combustion of Liquid Fuel Sprays", Combustion and Flame, Vol. 120, pp. 479–491, 2000.

35. Bachalo W.D., "Spray Diagnostic Techniques and the Application to the Study of Spray Interactions with Turbulent Flows", in Mechanics and Combustion of Droplets and Sprays, Eds.: H.H. and N. Chigier, pp. 297–327, Begell House, New York, 1995.

36. Eaton, J.K. and Fessler, J.R., "Preferential Concentration of Particles by Turbulence", International Journal of Multiphase Flow, Vol. 20, pp. 169–209, 1994.

37. Wood, A.M., Hwang, W. and Eaton, J.K., "Preferential Concentration of Particles in Homogeneous and Isotropic Turbulence", International Journal of Multiphase Flow, Vol. 31, pp. 1220–1230, 2005.

38. Beard P.J., Bissieres D., Lavregne G.D. and Rompteaux, A.A., "Experimental and Numerical Studies of Droplet Turbulent Dispersion in Two-Phase Flows", Numerical Methods in Multiphase Flows, Vol. 185, pp 15–22, 1994.

39. Wark C., Eickmann K., Richards C., "The Structure of an Acoustically Forced, Reacting Two-Phase Jet", Combustion and Flame, Vol. 120, pp. 479–491, 2000.

40. Dan T., Takagashi S., Senda J., Fujimoto H., "Organised Structure and Motion in Diesel Sprays", SAE Paper 970641, 1997.

41. Siebers D.L., "Liquid Phase Fuel Penetration in Diesel Sprays" SAE Paper 980809, 1998.

42. Siebers D.L., "Scaling Liquid-Phase Fuel Penetration in Diesel Sprays Based on Mixing-Limited Vaporisation" SAE Paper 1999-01-0528, 1999.

43. Behringer, M.K., Aleiferis, P.G., Oudenijeweme, D. and Freeland, P., "Spray Formation from Spark-Eroded and Laser-Drilled Injectors for DISI Engines with Gasoline and Alcohol Fuels", SAE Paper 2014-01-2745, 2014.

44. Yaws, C.L., Yaws' Handbook of Thermodynamic and Physical Properties of Chemical Compounds", Knovel, 2003.

LIST OF FIGURES

Figure 1. Schematic of injector and spray plumes.

1, 6   2, 5 3, 4   1, 2, 3   4, 5, 6

Figure 2. Schematic of injection vessel with Schlieren system (top) and combined Schlieren/planarMie scattering systems (bottom); components not to scale.

Gasoline	Backlight (Shadowgraph)	Schlieren	Planar Illumination (Mie)
20 °C, 1.0 bar			
120 °C, 0.5 bar			
120 °C, 5.0 bar			
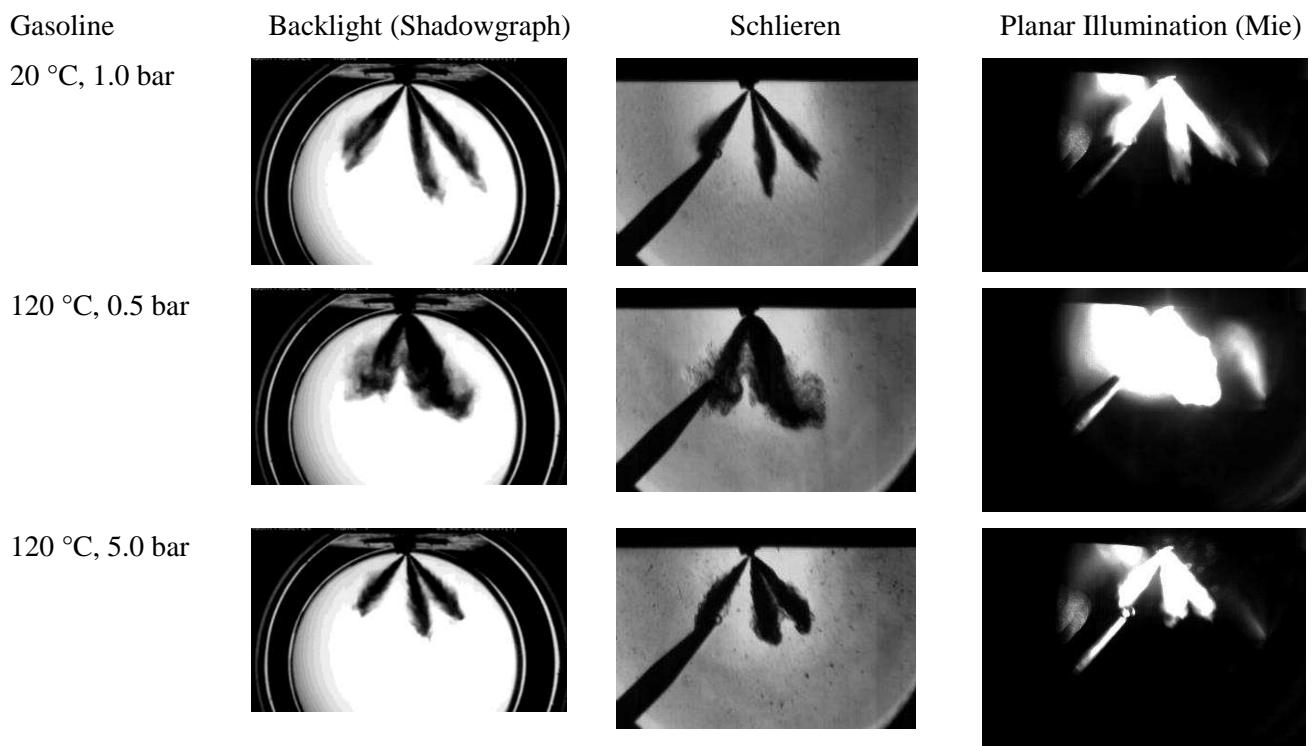
Figure 3. Spray comparison for different imaging techniques; gasoline, 777 μs ASOI.

iso-Octane	Backlight (Shadowgraph)	Schlieren	Planar Illumination (Mie)
20 °C, 1.0 bar			
120 °C, 0.5 bar			
120 °C, 5.0 bar			
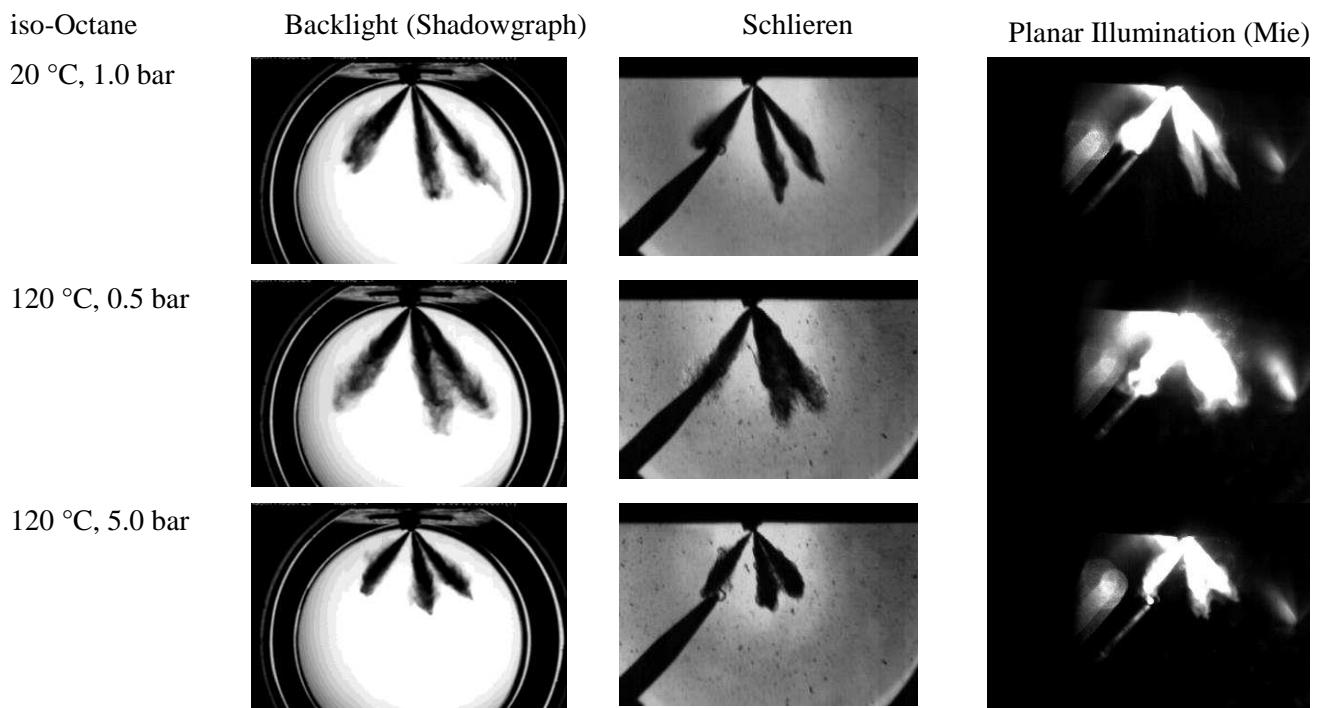
Figure 4. Spray comparison for different imaging techniques; iso-octane, 777 μs ASOI.
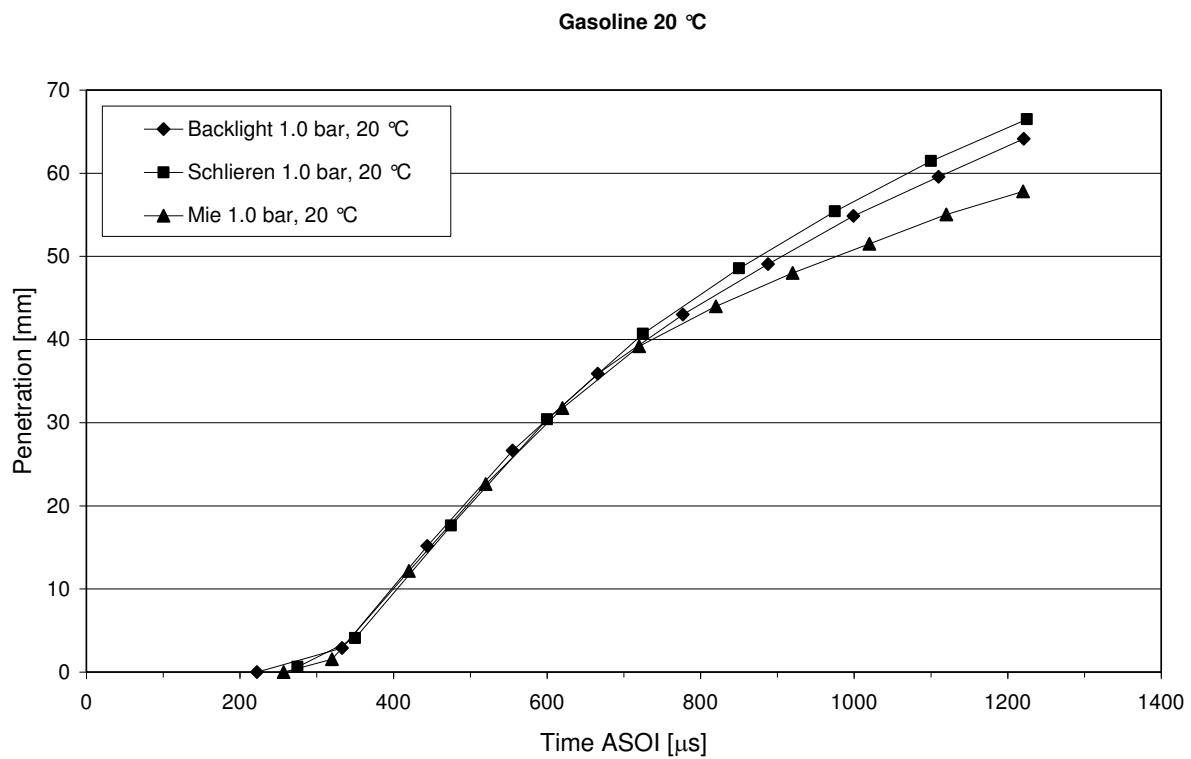
Gasoline 20 ℃

Figure 5. Penetration curves for gasoline, 20 °C, 1 bar.
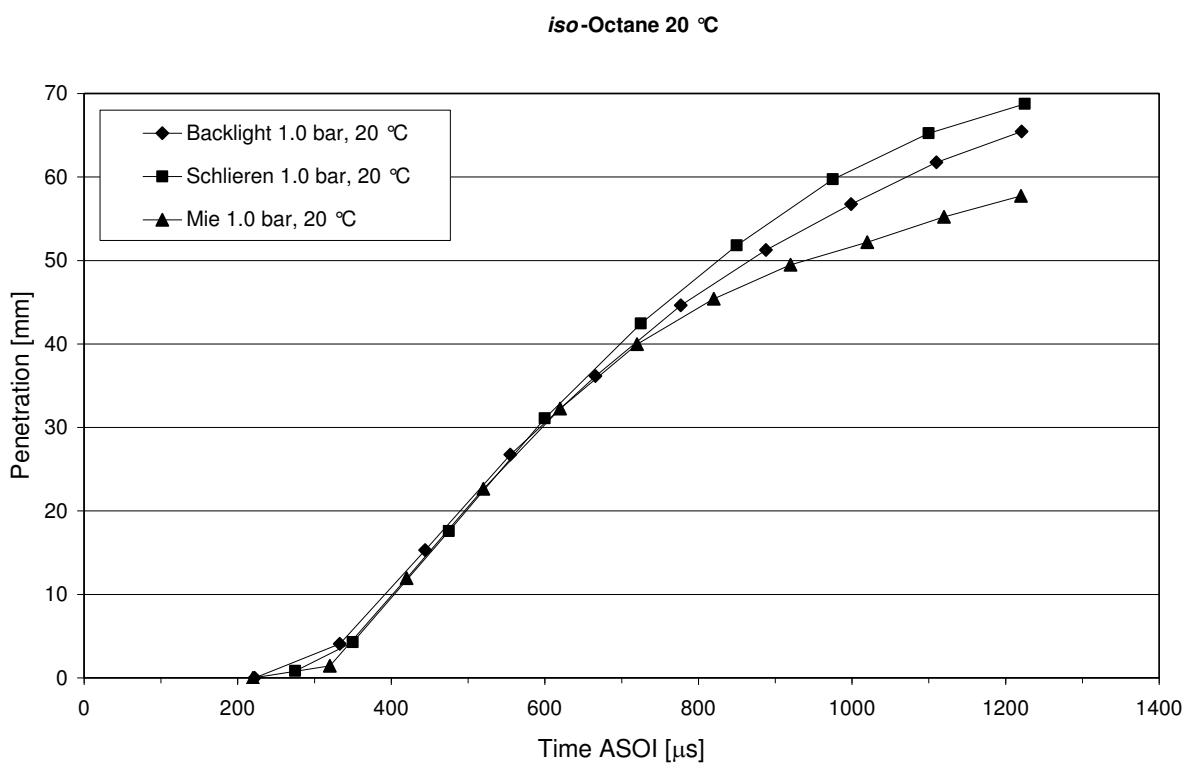
***iso*-Octane 20 ℃**

Figure 6. Penetration curves for iso-octane, 20 °C, 1 bar.

Gasoline 90 ℃
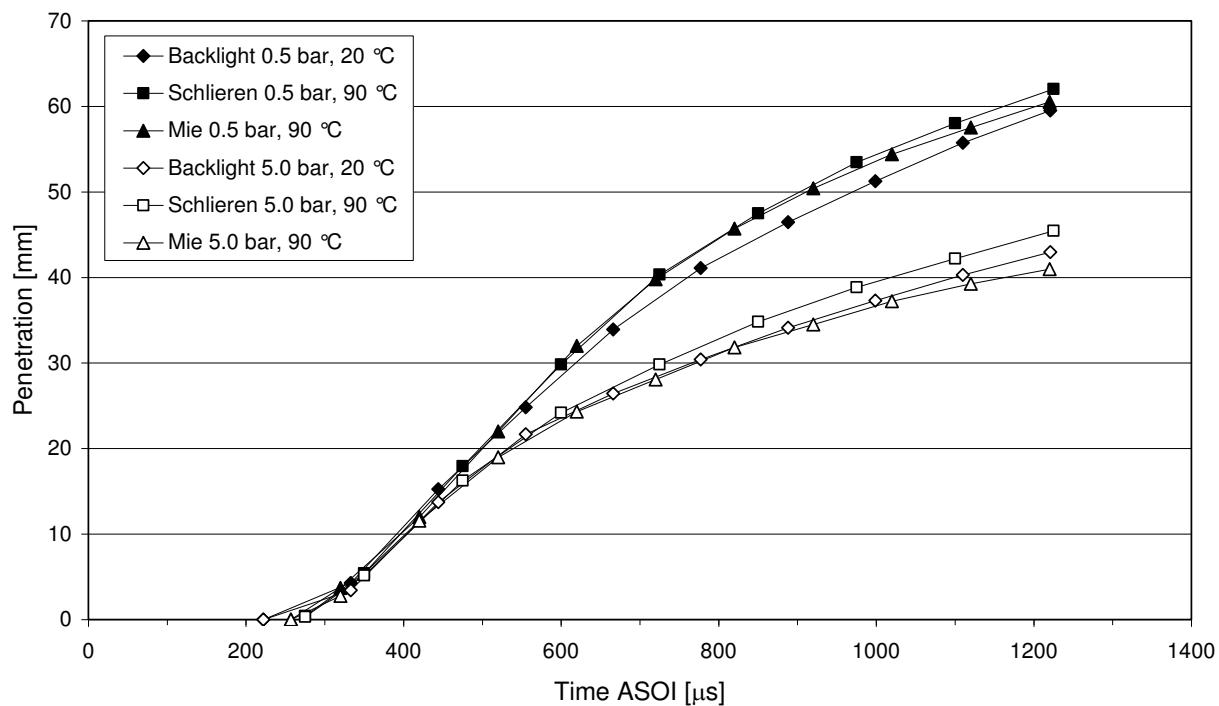
Figure 7. Penetration curves for gasoline, 90 °C.

Gasoline 120 ℃
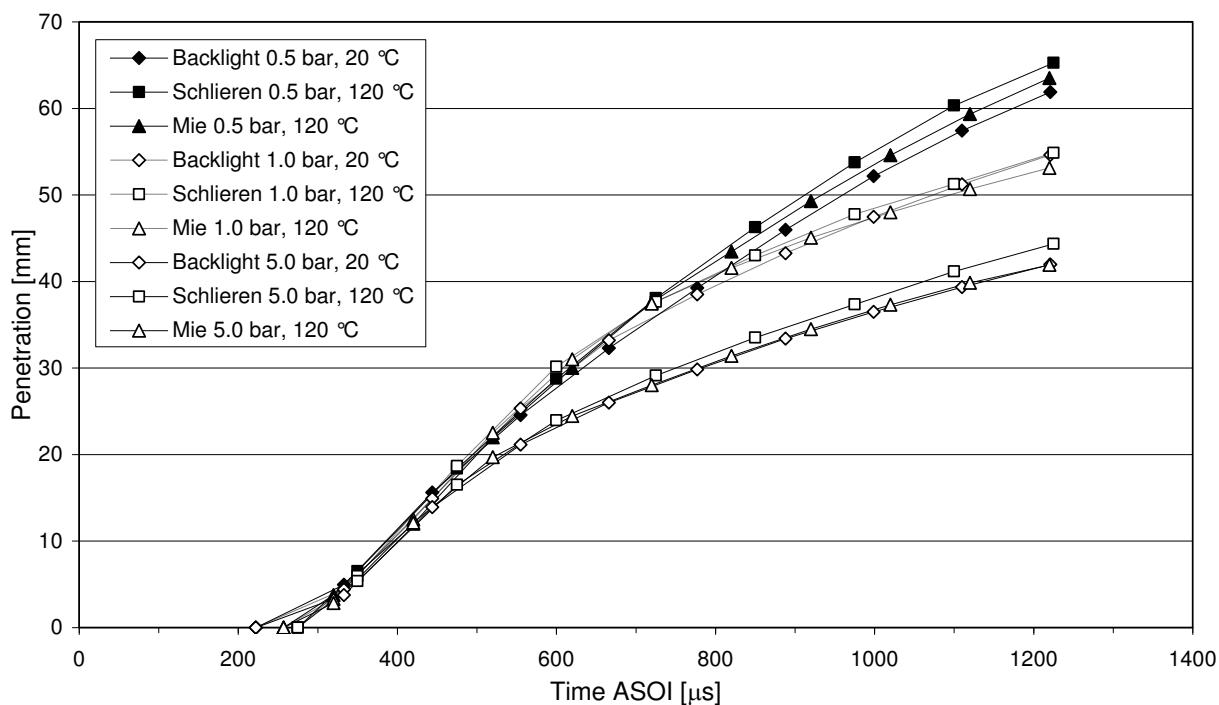
Figure 8. Penetration curves for gasoline, 120 °C.
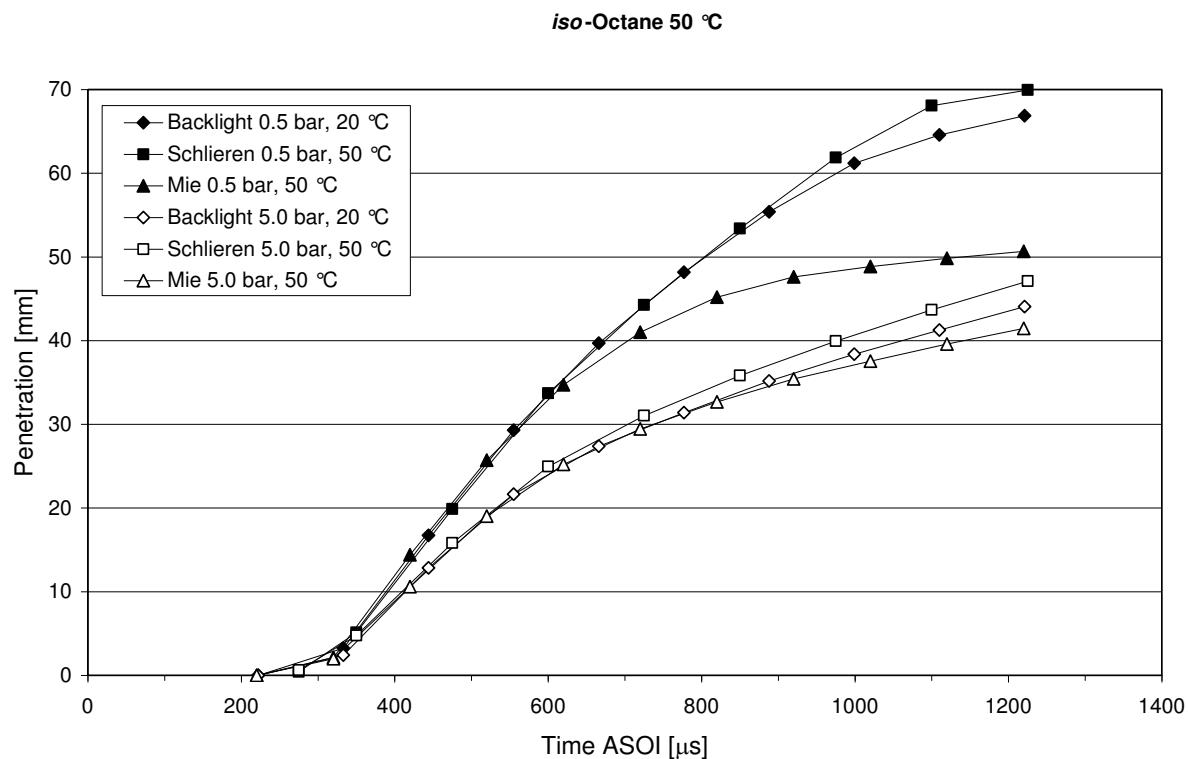
Figure 9. Penetration curves for iso-octane, 50 °C.
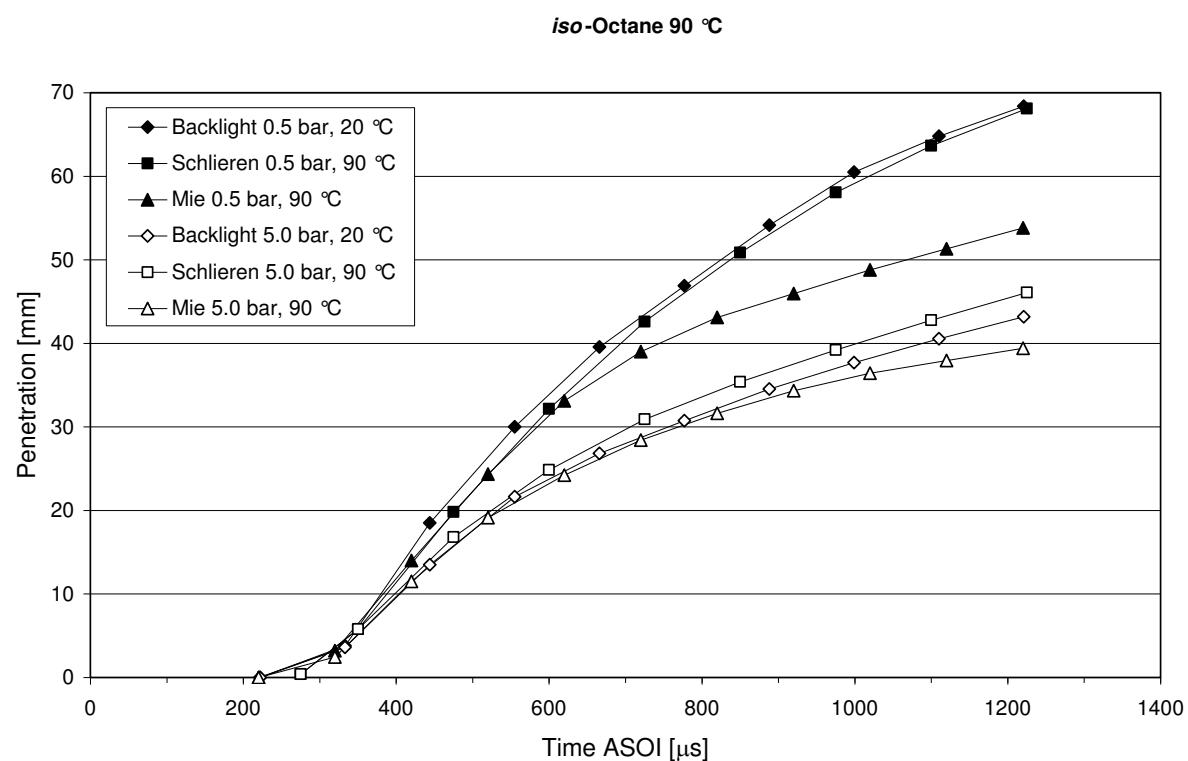
Figure 10. Penetration curves for iso-octane, 90 °C.
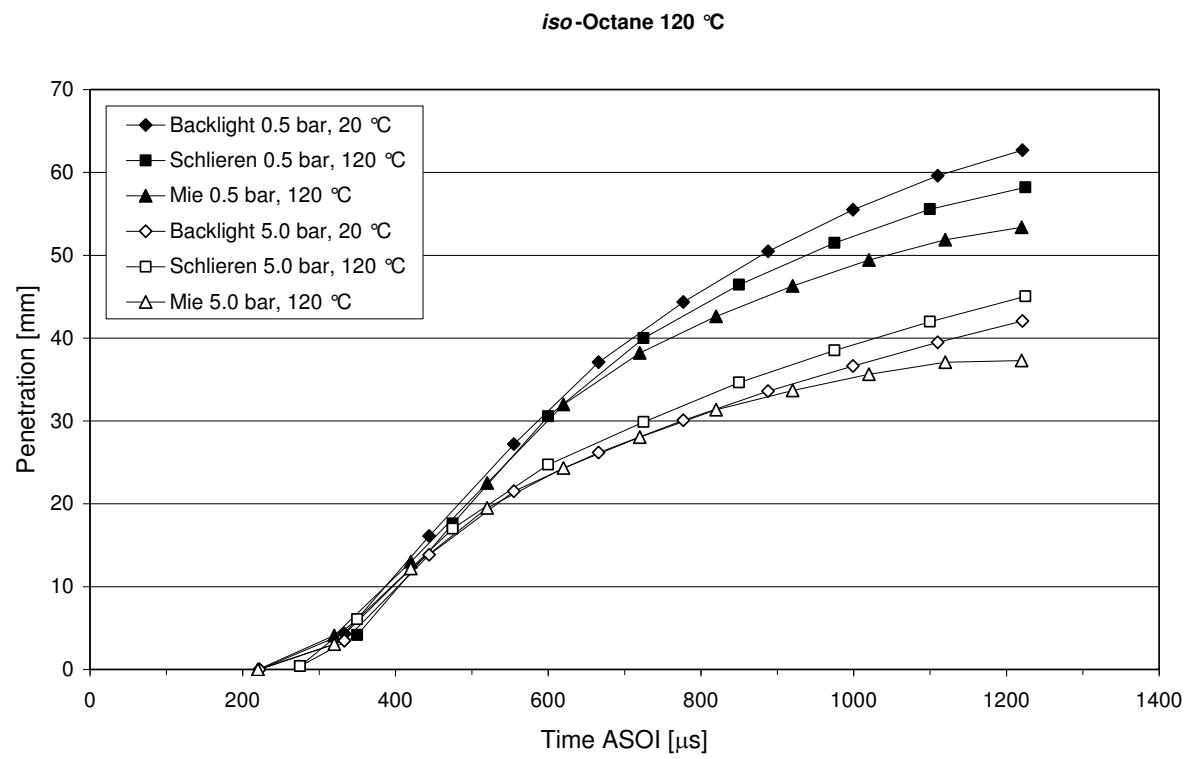
Figure 11. Penetration curves for iso-octane, 120 °C.

Gasoline
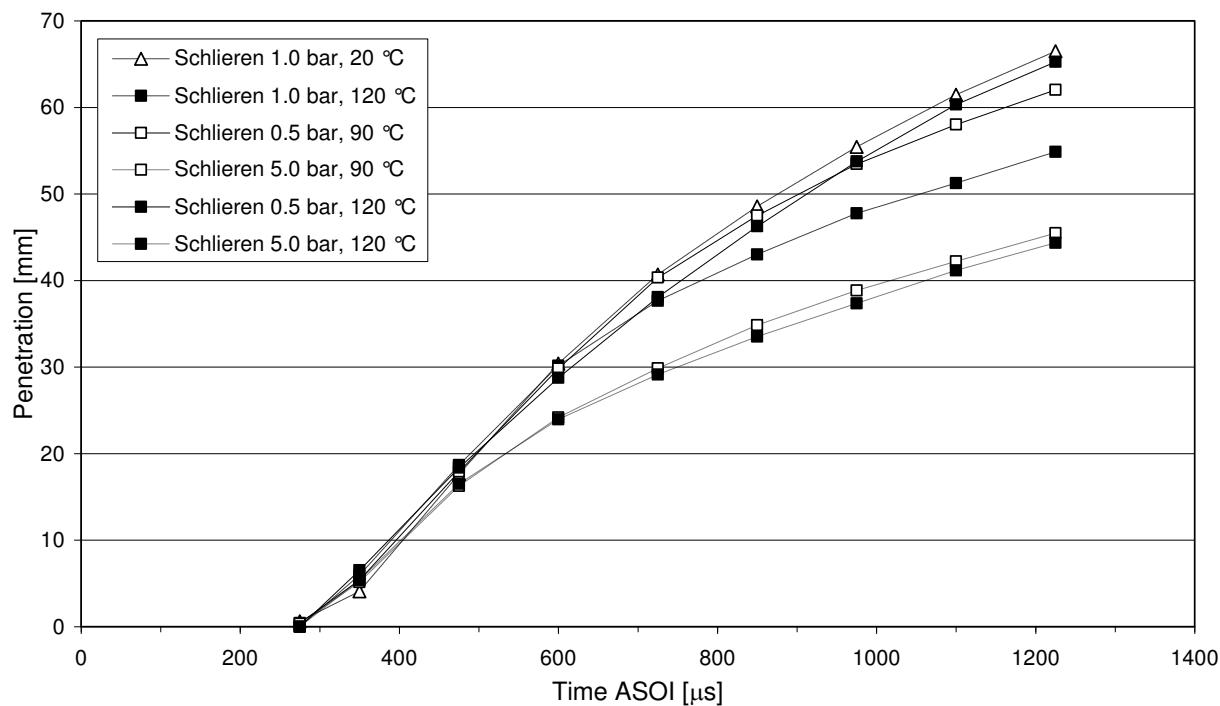
Figure 12. Penetration curves for gasoline (Schlieren).

***iso*-Octane**
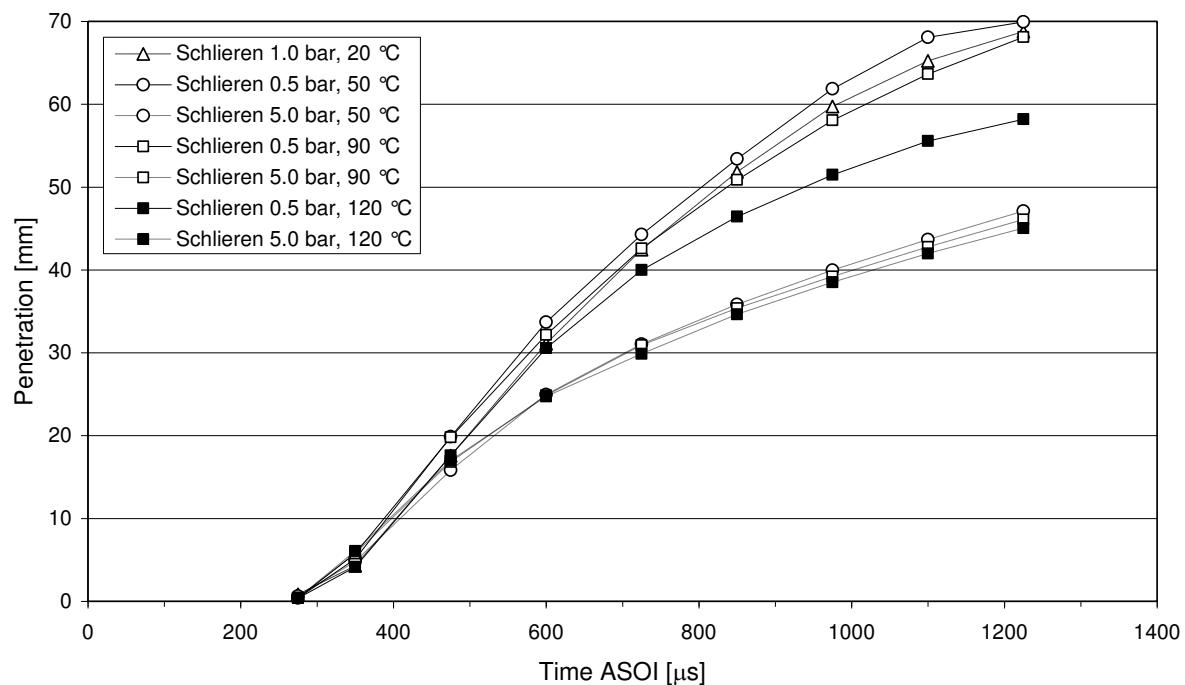
Figure 13. Penetration curves for iso-octane (Schlieren).
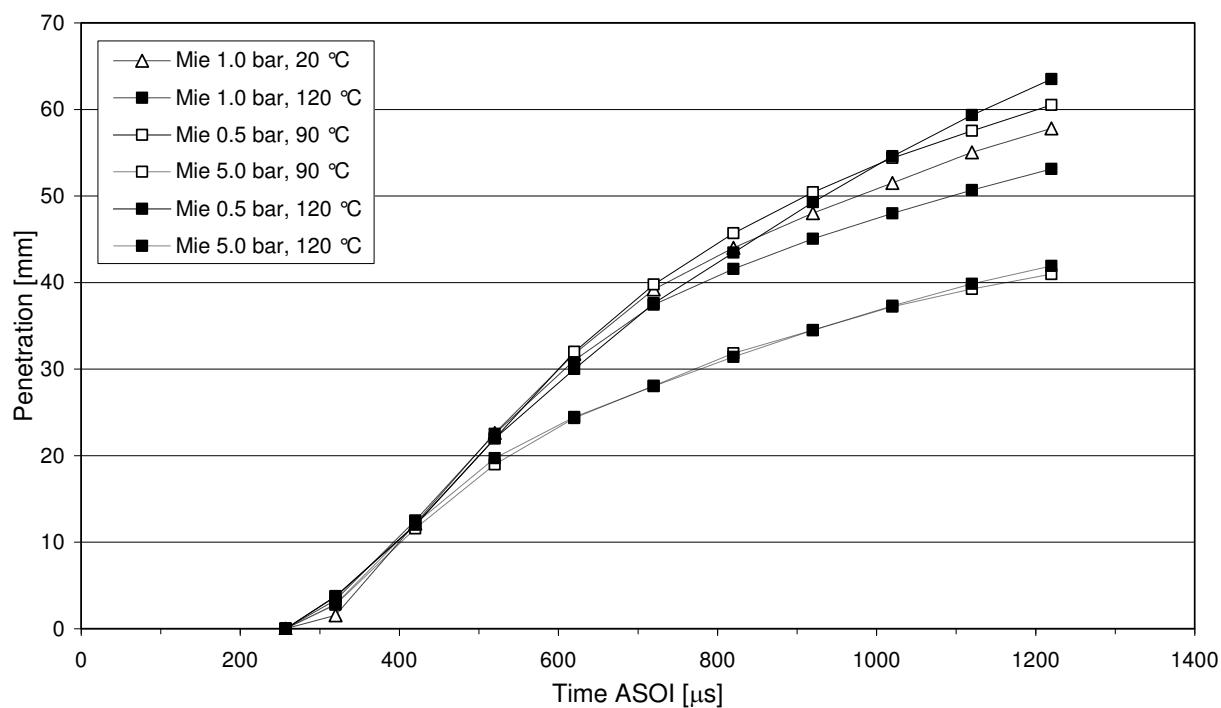
Figure 14. Penetration curves for gasoline (Mie).
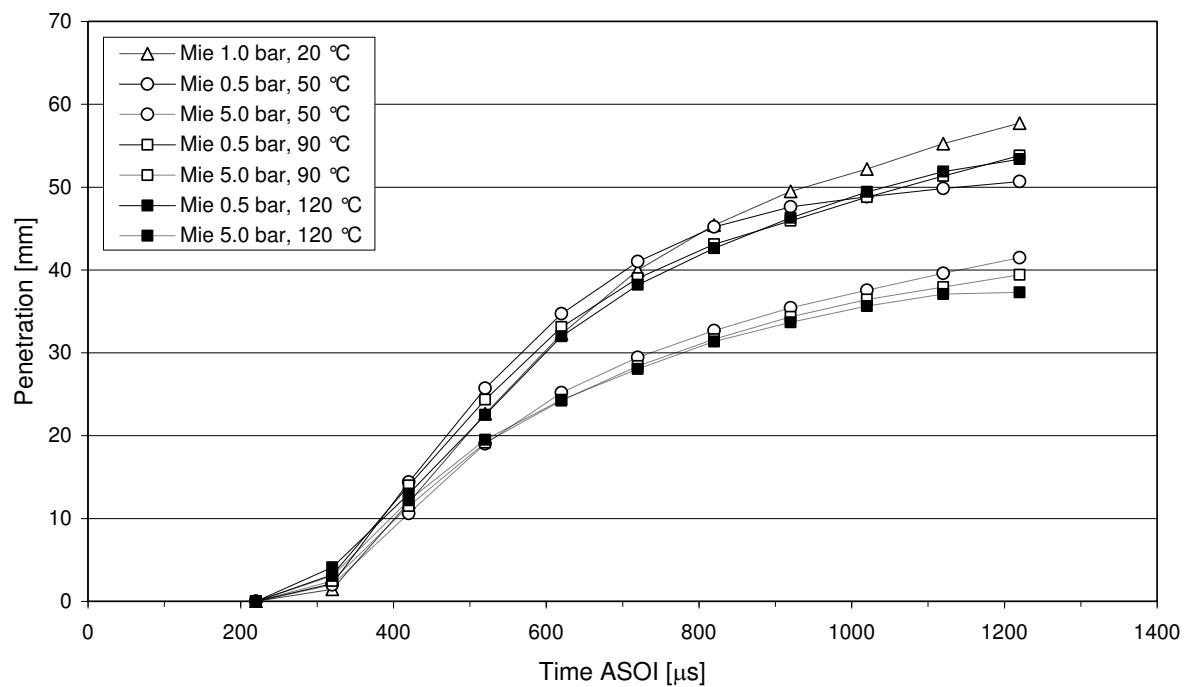
Figure 15. Penetration curves for iso-octane (Mie).

Time ASOI [µs]	Image	u′ = 0 m/s	u′ = 2 m/s	u′ = 4 m/s
	Typical			
475	Mean			
	RMS			
	Typical			
725	Mean			
	RMS			
	Typical			
975	Mean			
	RMS			
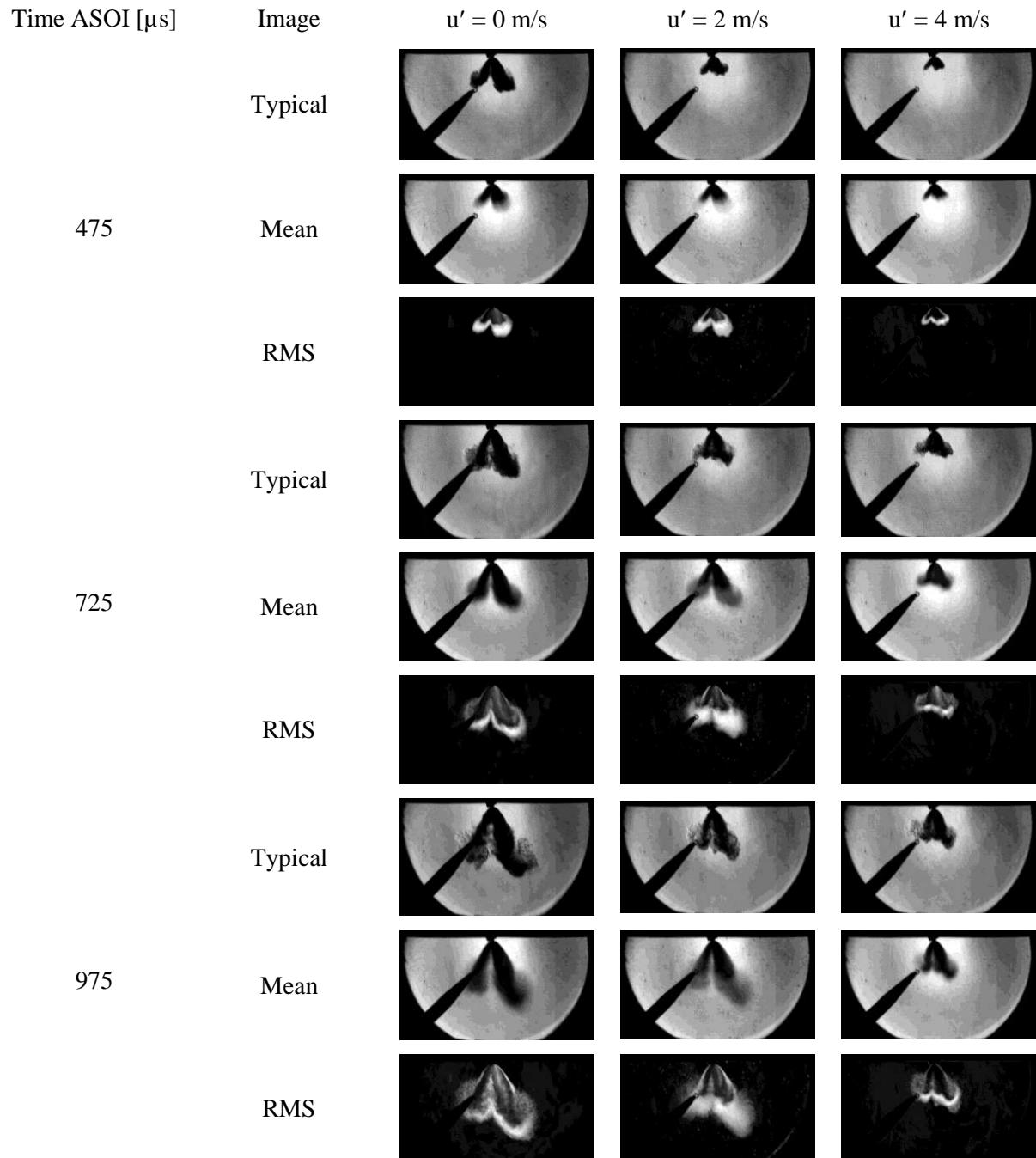
Figure 16. Effect of turbulence on spray development; gasoline, 120 °C, 0.5 bar (collapsed spray).

Time ASOI [µs]	Image	u′ = 0 m/s	u′ = 2 m/s	u′ = 4 m/s
	Typical			
475	Mean			
	RMS			
	Typical			
725	Mean			
	RMS			
	Typical			
975	Mean			
	RMS			
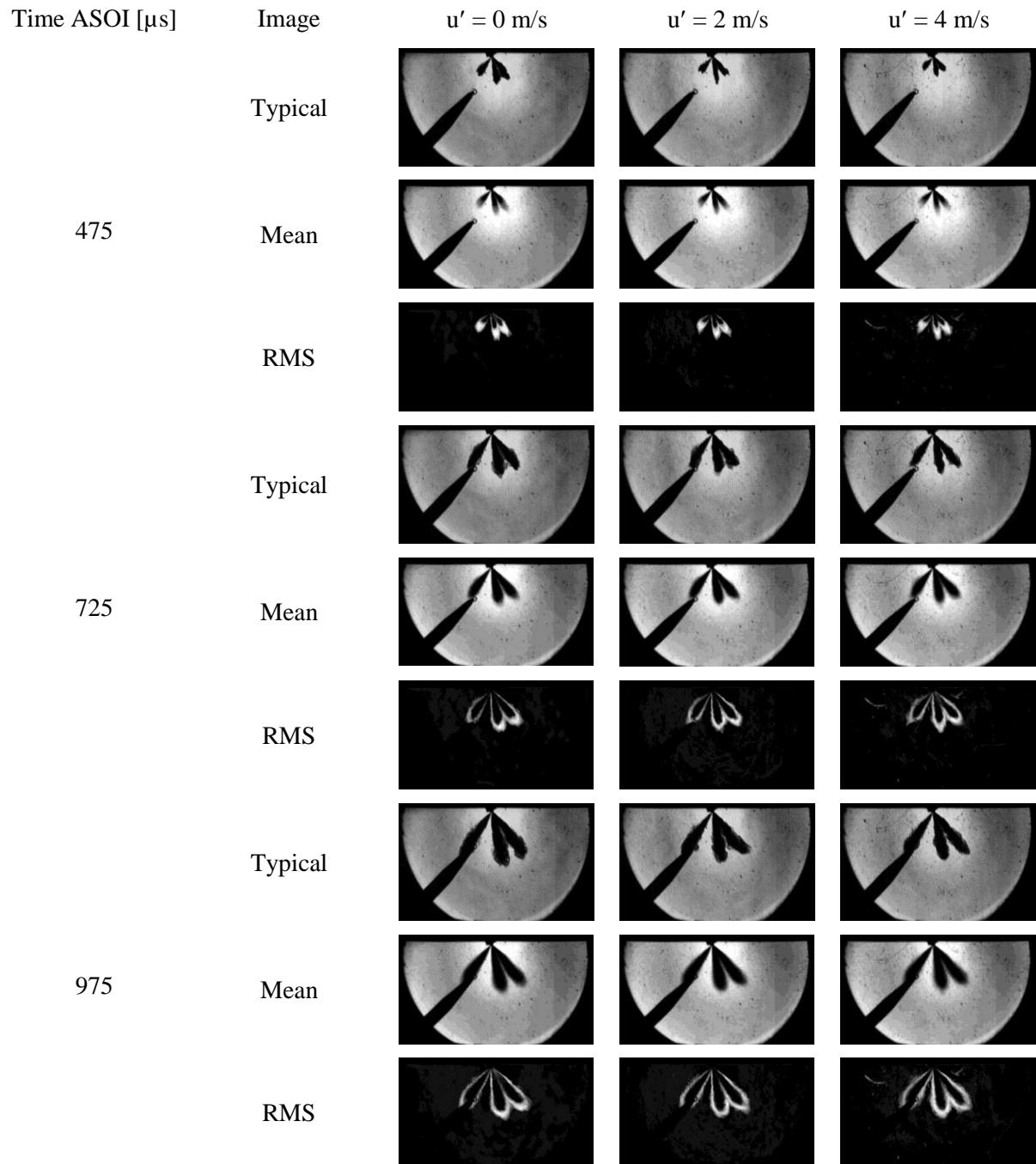
Figure 17. Effect of turbulence on spray development; gasoline, 120 °C, 5.0 bar (uncollapsed spray).
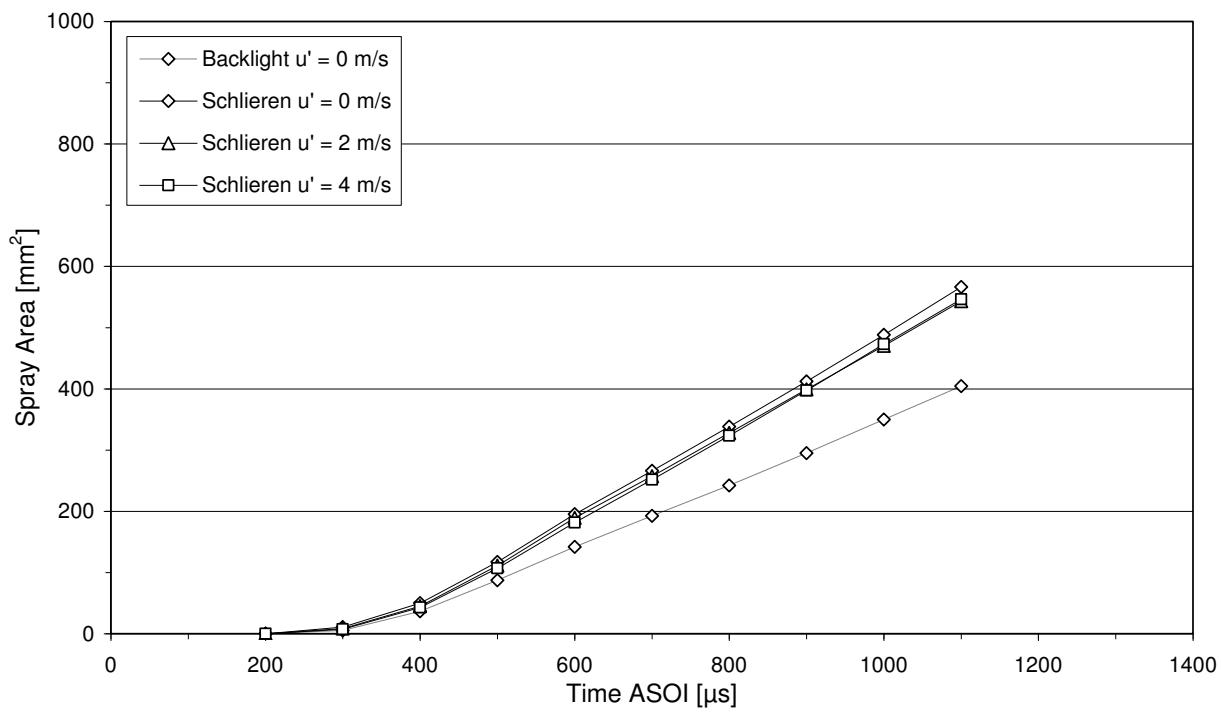
Figure 18. Effect of turbulence on spray area; gasoline, 120 °C, 5.0 bar.

Gasoline 120 ℃, 0.5 bar

Figure 19. Effect of turbulence on spray area; gasoline, 120 °C, 0.5 bar.

34

Gasoline 120 °C, 5.0 bar

Figure 20. Effect of turbulence on spray penetration; gasoline, 120 °C, 5.0 bar.

Gasoline 120 °C, 0.5 bar
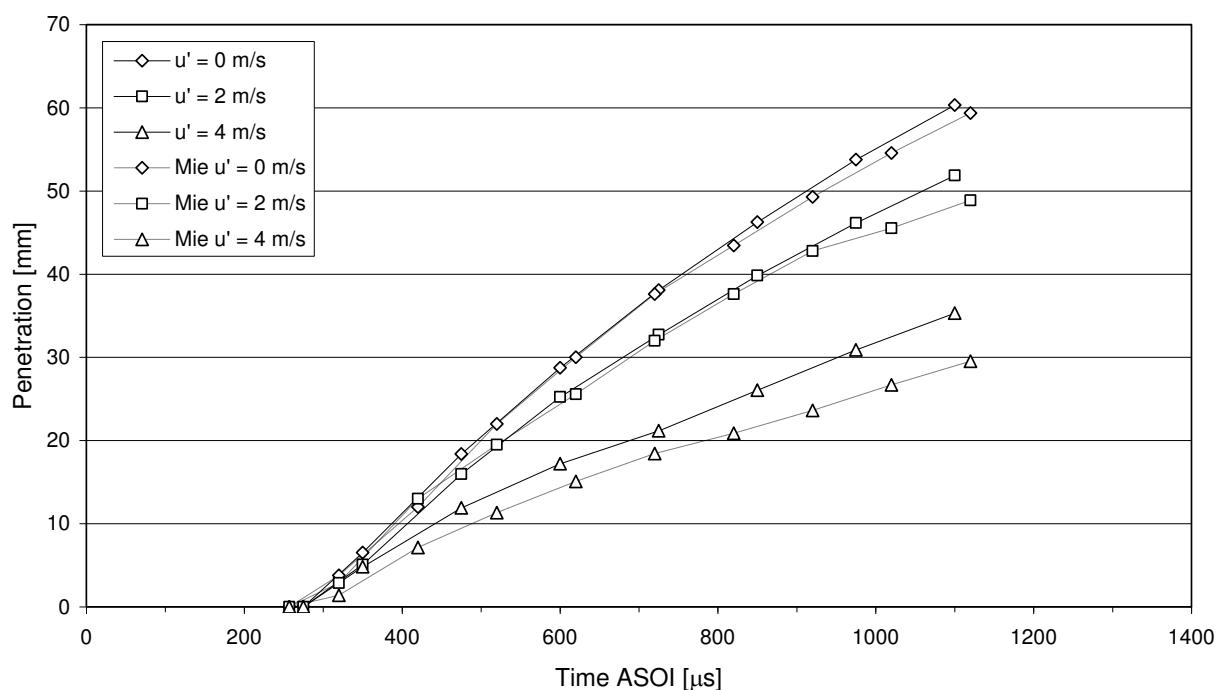
Figure 21. Effect of turbulence on spray penetration; gasoline, 120 °C, 0.5 bar.

Gasoline 120 ℃
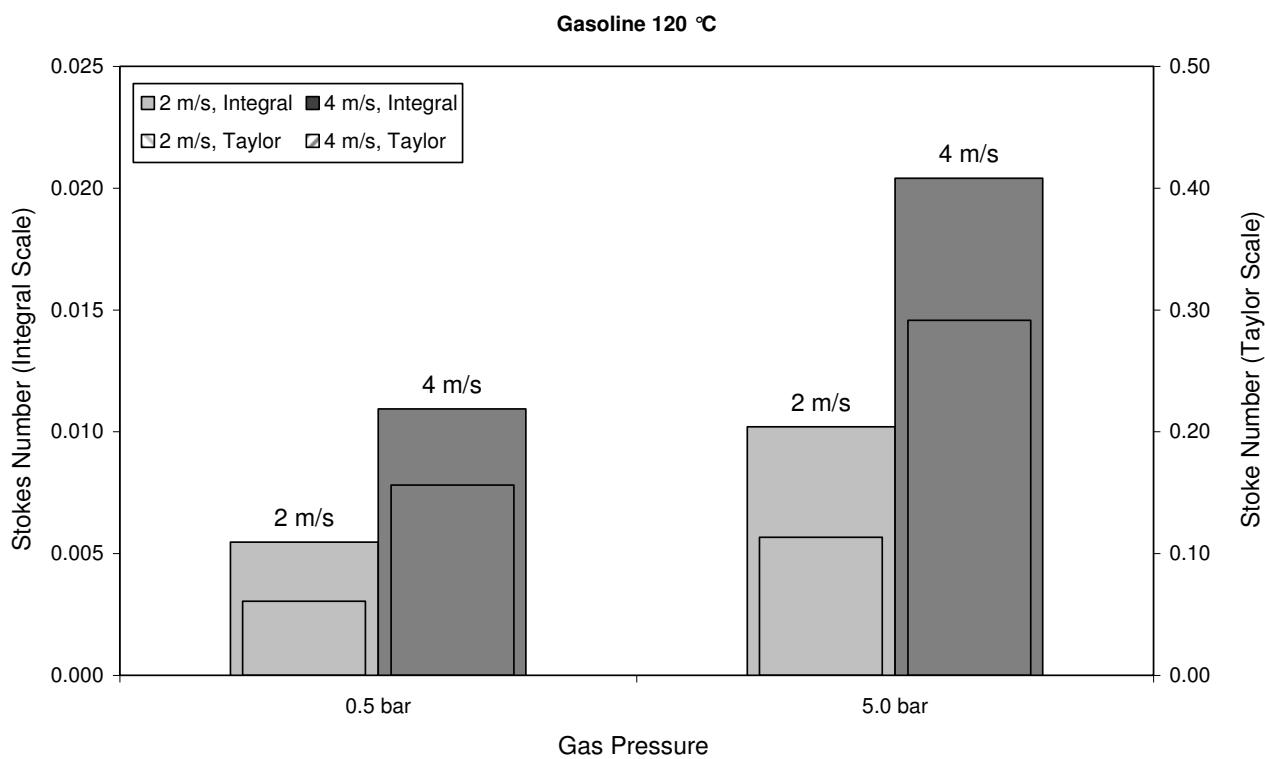
Figure 22. Stokes number.
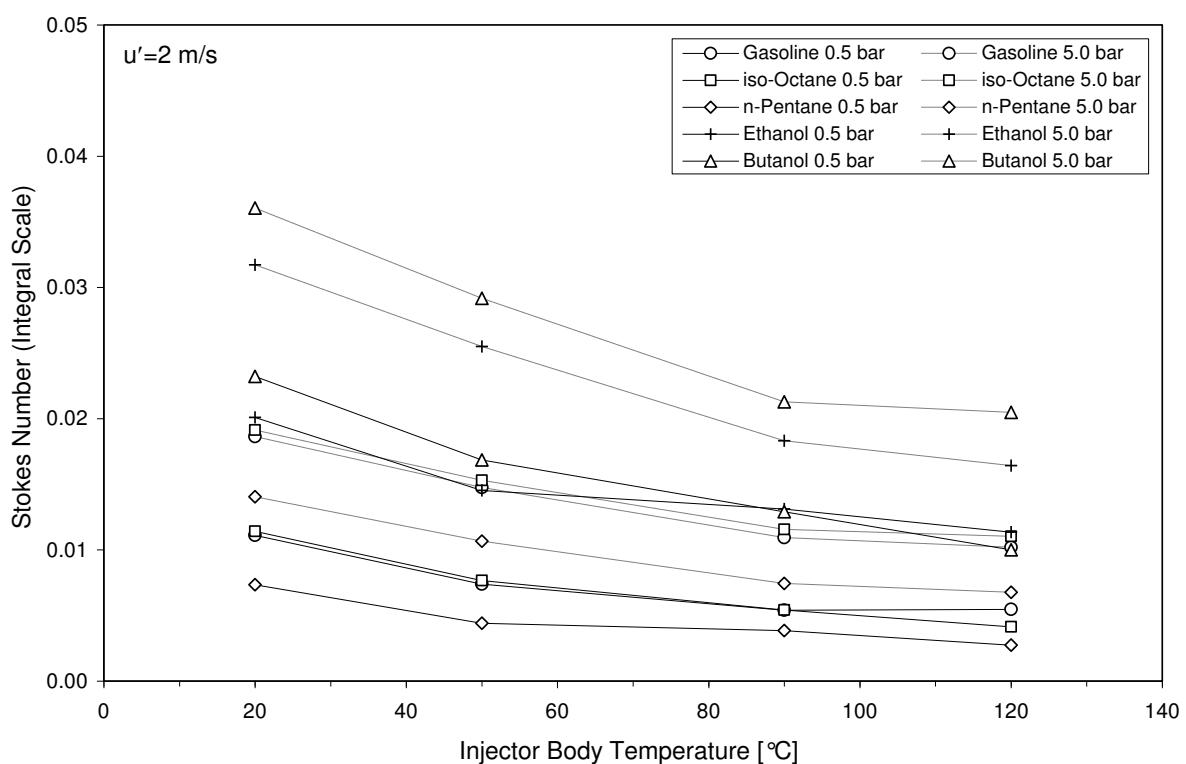
Figure 23. Integral scale Stokes number, u′=2 m/s, 0.5 bar and 5.0 bar, 20–120 °C.
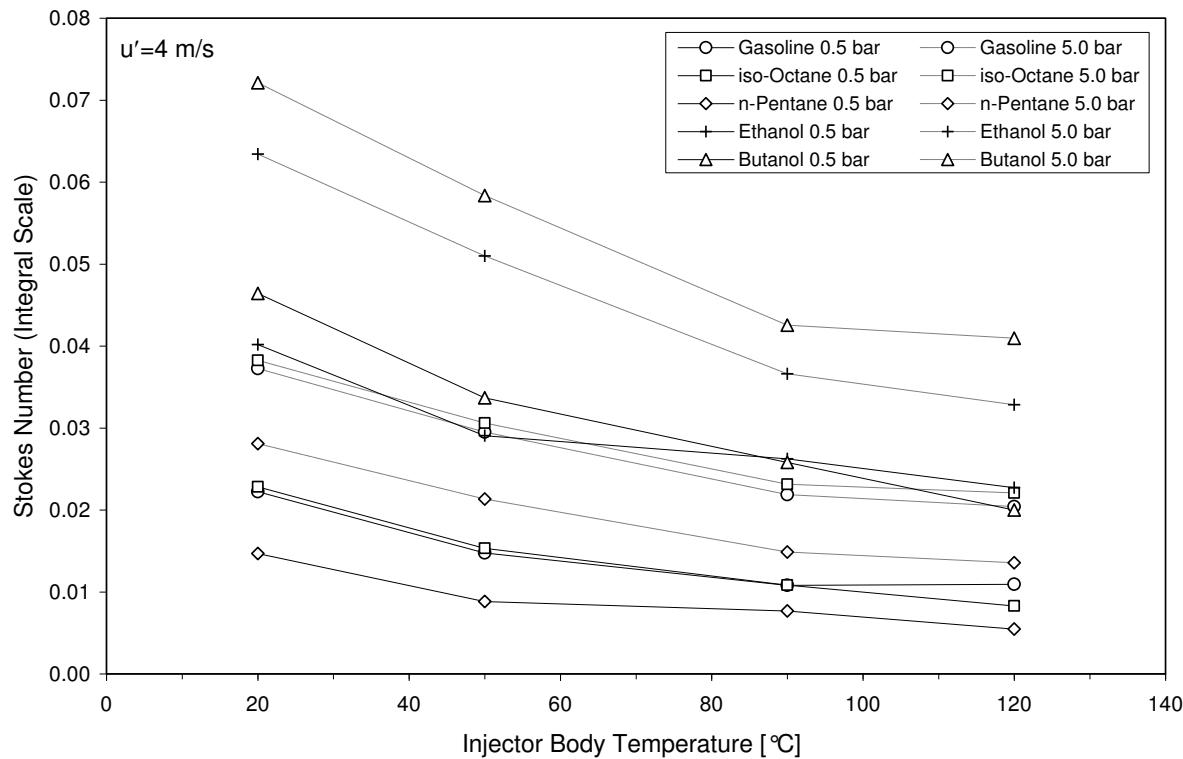
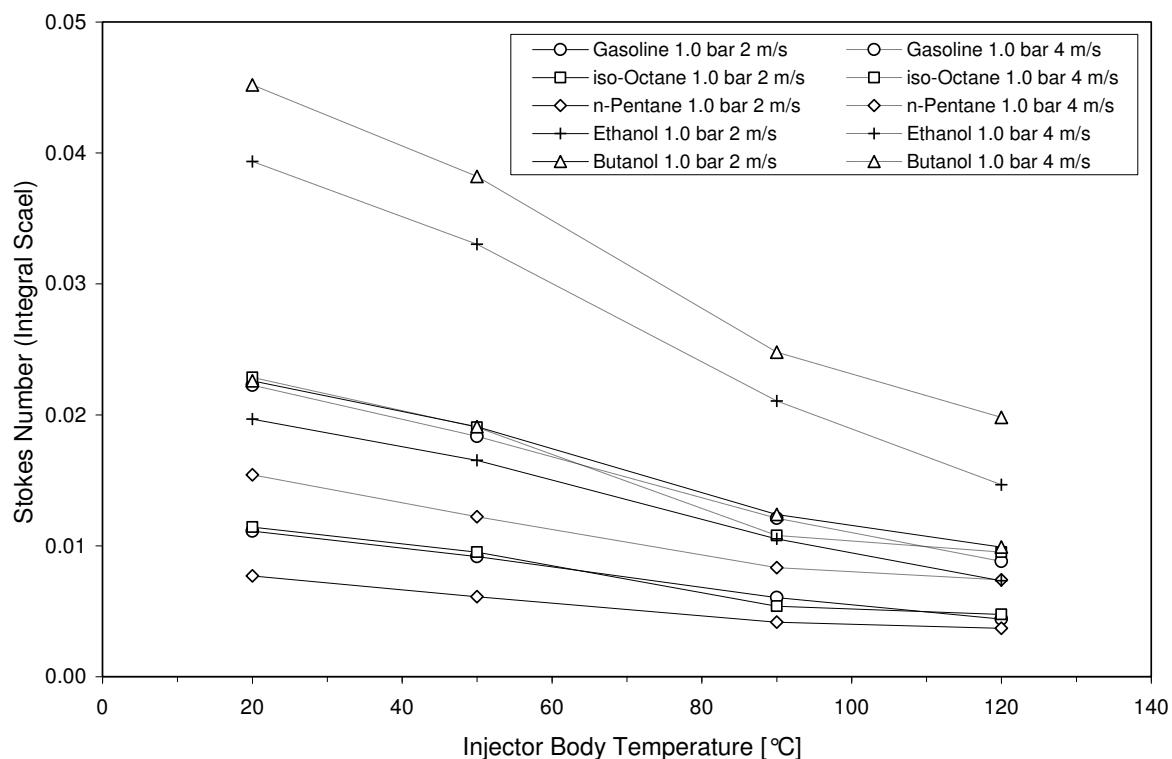**Figure 24. Integral scale Stokes number, u′=4 m/s, 0.5 bar and 5.0 bar, 20–120 °C.**

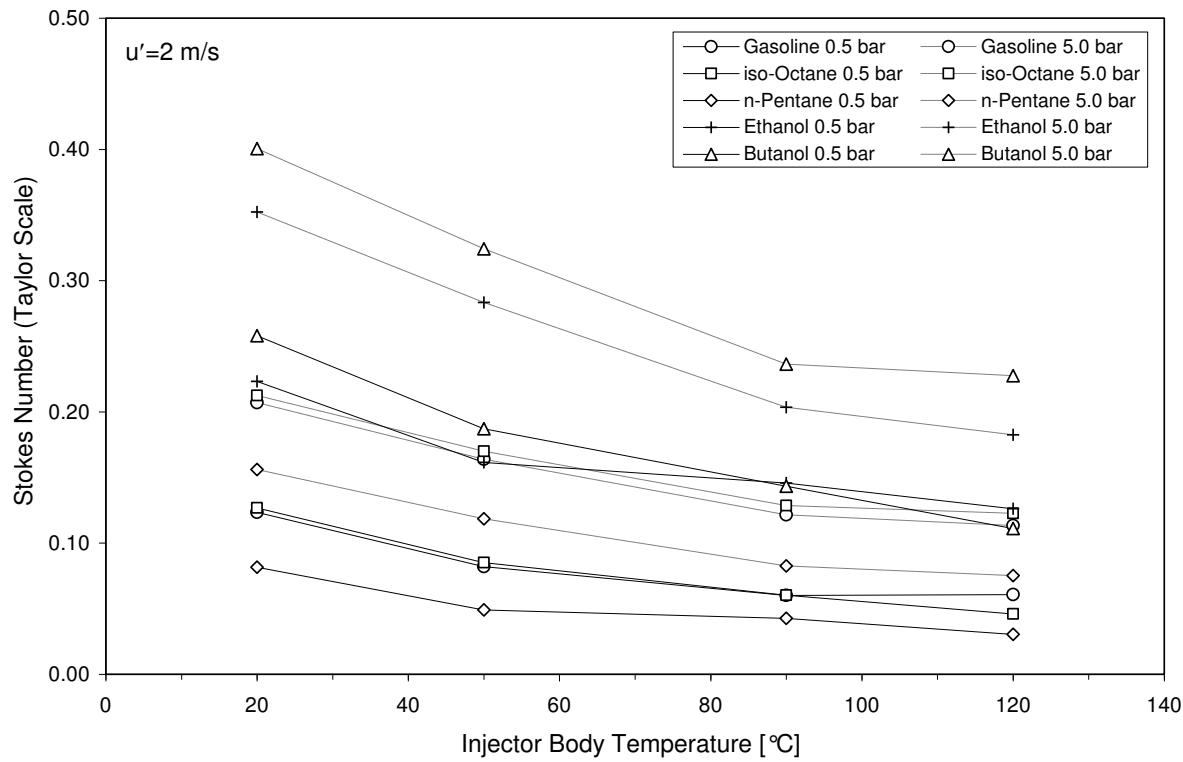**Figure 25. Integral scale Stokes number, u′=2–4 m/s, 1.0 bar, 20–120 °C.**

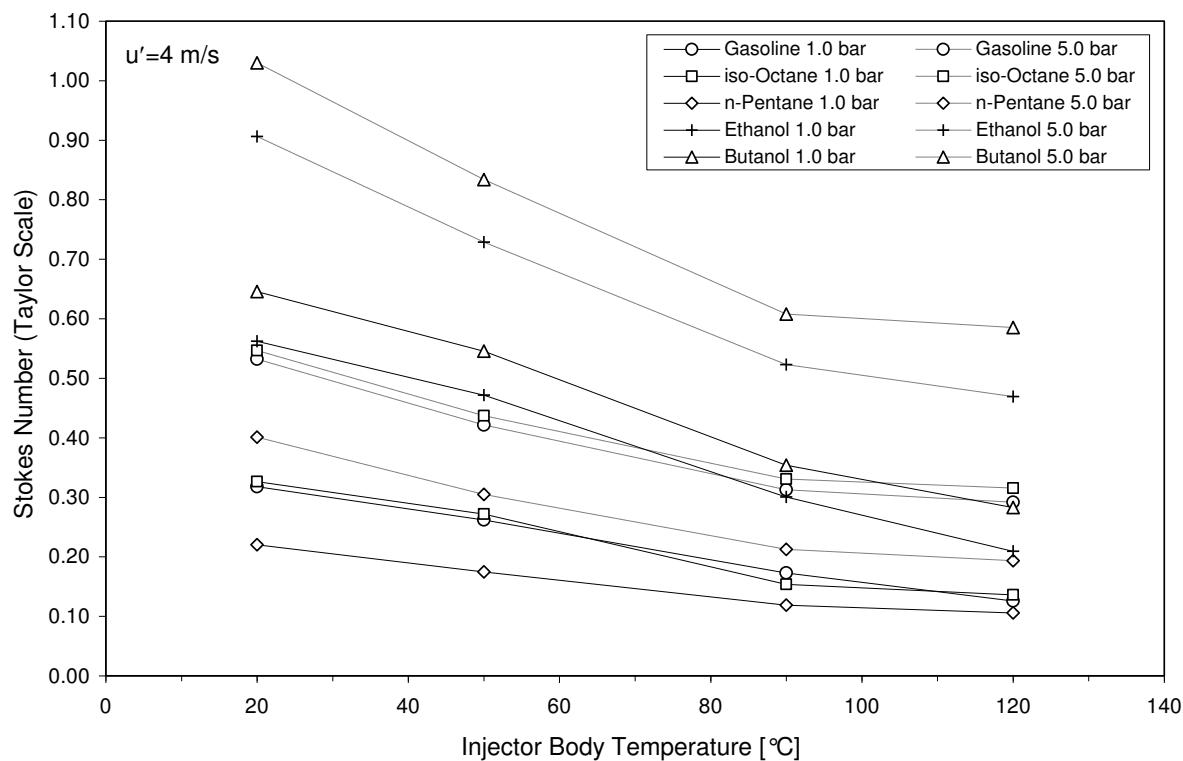**Figure 26. Taylor scale Stokes number, u′=2 m/s, 0.5 bar and 5.0 bar, 20–120 °C.**

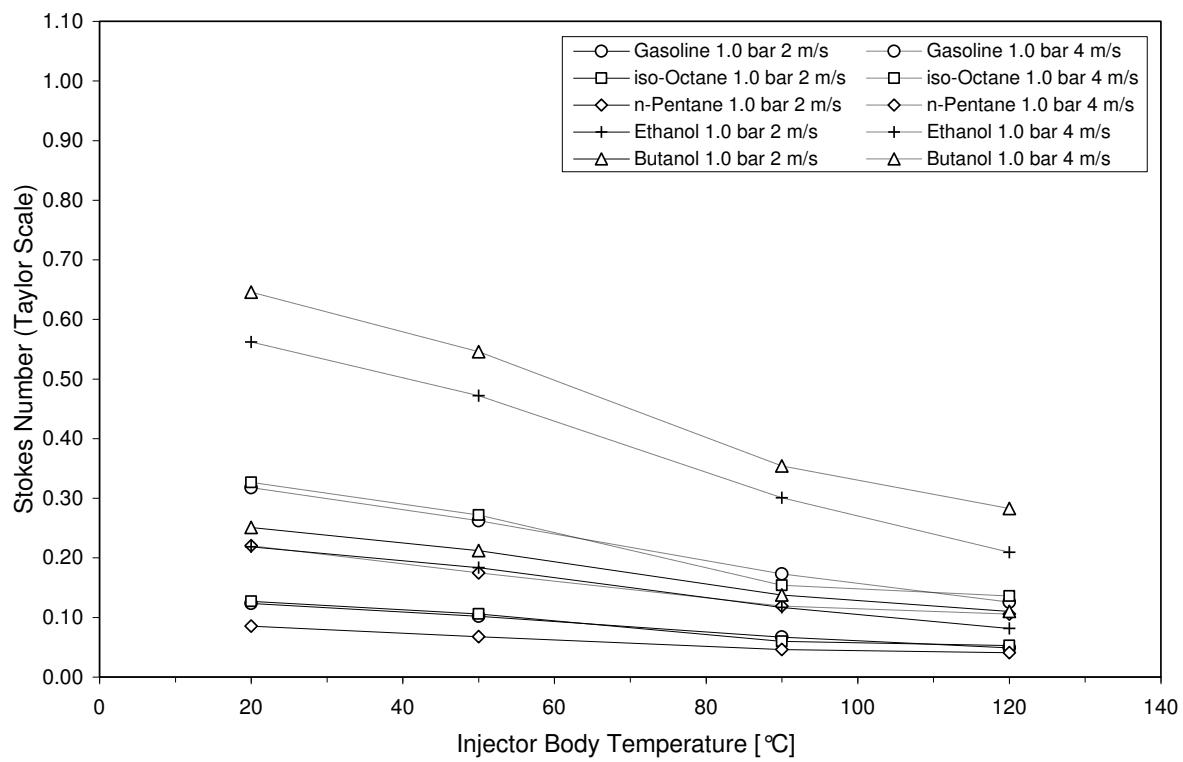**Figure 27. Taylor scale Stokes number, u′=4 m/s, 0.5 bar and 5.0 bar, 20–120 °C.**

38

Figure 28. Taylor scale Stokes number, u′=2–4 m/s, 1.0 bar, 20–120 °C.